2
Light Absorption by Water Molecules and Inorganic Substances Dissolved in Sea Water

The principal absorber of light and other electromagnetic radiation in seas and oceans is, of course, water as a chemical substance. Above all, this is due to the absolute numerical superiority of H_2O molecules over the molecules of all other substances contained in sea water: for every 100 H_2O molecules there are only 3–4 molecules of other substances, chiefly sea salt, but also dissolved organic substances, and the numerous suspended particles of mineral and organic matter, including phytoplankton cells and other live organisms. Although small in quantity, these various substances contained in sea water very significantly differentiate marine areas from the optical point of view. Water itself is a very strong absorber of electromagnetic radiation in the infrared (IR) region; thanks to this property it plays a prominent and indispensable role for life on Earth in that the ocean absorbs solar IR radiation and converts it into heat. This process leads directly to the warming of the ocean's surface waters, causing them to evaporate, and to the heating and circulation of the atmospheric air.

In this chapter we describe the mechanisms and spectra of light absorption by small molecules—principally water molecules—as well as the spectral absorption properties of liquid water, ice, and water vapor, and of the components of sea salt and other mineral substances dissolved in the water. Because of its exceptional significance in Nature, we give the water itself pride of place, describing its absorption spectra with respect not only to visible light but also to a wide spectrum of electromagnetic radiation, from the extremely short γ- and X-rays to long radio waves.

2.1 Light Absorption Spectra of Small Molecules such as Water: Physical Principles

As we stated in Chapter 1, the light absorption spectra of matter in its various states are determined by quantum changes in the atomic and molecular energies of that matter as a result of its having absorbed photons. Among these quantum processes we must include the energetic electronic transitions

in atoms, and also the electronic, vibrational, and rotational transitions in molecules, all of which in fact take place simultaneously. We can explain these quantum changes of energy with respect to a molecule most simply if we examine the energy states of a free molecule.

The total energy of a freely moving molecule $E_M\ (\Lambda,\upsilon,J)$ consists of the temperature-dependent energy of its translational motion E_{TR}, the energy of its rotation about its various axes of symmetry $E_{ROT}(J)$, the vibrational energy of its atoms around its equilibrium position $E_{VIB}(\upsilon)$, and the energy of its electrons $E_E(\Lambda)$, where J, υ, Λ, are respective quantum numbers. We can thus write down this total energy as the sum of these component energies:

$$E_M\ (\Lambda,\upsilon,J) = E_E(\Lambda) + E_{VIB}(\upsilon) + E_{ROT}(J) + E_{TR}. \tag{2.1}$$

The first three—quantized—energy constituents on the right-hand side of Equation (2.1) depend on the extent to which the molecule is excited. In other words, they take discrete values, strictly defined by the given quantum (energy) state of the molecule. The energy states of a simple molecule (e.g., H_2O, CO_2) are defined by the rotational energy (the quantum number or numbers J), the vibrational energy (the quantum number or numbers υ), and the electronic energy (given by the quantum number Λ), defining the absolute value of the projection of the angular momentum on to the molecule's axis.

The absorption or emission by a molecule of a photon of energy $E_{h\nu} = h\nu$ invariably involves its transition from one quantum state, described by quantum numbers Λ, υ, J, to another quantum state, described by Λ', υ', J' (in the general case all three quantum numbers change) in accordance with the allowed quantum mechanical selection rules. The energy of this photon is then equal to the difference between the molecule's energies in these two states and can be written as

$$\begin{aligned} E_{h\nu} = E_M(\Lambda,\upsilon,J) - E_M(\Lambda',\upsilon',J') = \Delta E_E(\Lambda\rightarrow\Lambda') + \\ \Delta E_{VIB}(\upsilon\rightarrow\upsilon') + \Delta E_{ROT}(J\rightarrow J') + \Delta E_{TR}. \end{aligned} \tag{2.2}$$

So it is the sum of the increments (or losses) of energy of the several components in these two states (initial and final), that is, the increments of electronic (ΔE_E), vibrational (E_{VIB}), rotational (E_{ROT}), and translational (E_{TR}) energy. The increments of these first three energy components of the molecule following the absorption of a photon give rise to the three principal types of absorption band, which we discuss presently. The transition of a molecule from one electronic state to another (the selection rule for such transitions is $\Delta\Lambda = 0, \pm1$) usually brings about changes in the vibrational state (selection rule: $\Delta\upsilon = \pm1, \pm2, \ldots$) and the rotational state of the molecule (selection rule: $\Delta J = 0, \pm1$) as well. A transition during which all three types of molecular energy change as a result of the absorption (or emission) of energy gives rise to an *electronic-vibrational-rotational* spectrum of the absorption of electromagnetic wave energy. This is a band spectrum with a highly complex structure consisting of very many spectral lines forming two or three branches

denoted R($\Delta J = 1$), P($\Delta J = -1$), and Q($\Delta J = 0$). The lines of these branches lie in the ultraviolet and visible regions of the electromagnetic waves spectrum (in the case of water only in the ultraviolet).

In certain electronic states, a molecule may, as a result of allowed vibrational-rotational energy transitions, change only its vibrational and rotational energy. Transitions of this kind give rise to vibrational-rotational absorption spectra as a result of the absorption (or emission) of relatively low-energy quanta, that is, from the infrared region of electromagnetic waves.

If a molecule is not symmetrical or has a dipole moment other than zero (like the water molecule, for example), then as a result of the absorption (or emission) of energy quanta from the microwave or radiowave ranges, its rotational energy may change without the electronic or vibrational states being affected. What we then have is a rotational absorption band.

This simplified picture of a molecule's internal energy changes reflects the structural complexity of a molecular spectrum of the absorption (or emission) of electromagnetic wave energy. In this chapter we present the theoretical foundations underlying this process, which are essential for understanding the structure of the light absorption spectra of water molecules; it also helps in understanding the absorption band structures of other small molecules. A more detailed treatment of the subject can be found in the numerous monographs on molecular physics, spectroscopy, and quantum mechanics and chemistry, for example, Barrow (1969), Herzberg (1950, 1992), Banwell (1985), Hollas (1992), Haken and Wolf (1995, 1998, 1996, 2002), Kowalczyk (2000), and Linne 2002, to mention but a few. The following works, dealing specifically with the various properties of water, in particular the interaction of water molecules with electromagnetic radiation, are also deserving of attention: Eisenberg and Kauzmann (1969), Lemus (2004), and Chaplin (2006), again, to mention just three. Moreover, Bernath (2002) provides a detailed review of the subject literature, and in the course of this chapter we cite yet other works.

2.1.1 Vibrational-Rotational Absorption Spectra

Water molecules appear to be the most important ones involved in the process of solar energy absorption because of their untold numbers in the ocean and atmosphere, as well as their crucial optical properties. Of particular significance in Nature is the very strong absorption by water molecules of infrared radiation (IR), as a result of transitions between the vibrational-rotational energy states in these molecules. According to our estimates, this IR absorption by water molecules is equivalent to some 60% of the total solar radiation energy absorbed in the Earth's epigeosphere (i.e., around 70% of the energy absorbed in the atmosphere and some 50% of the energy absorbed in the sea).

How the water molecule interacts with electromagnetic radiation depends closely on its physical properties. Important in this respect are its geometrical

parameters (the positions of the atoms vis-à-vis one another and the configuration of electrons), as well as its dynamic, electrical, and magnetic properties. Table 2.1 lists many of these properties that are directly related to the optical properties of water. We refer frequently to this table in the present (2.1) and the next section (2.2).

As we can see in Table 2.1 (items (1) to (3)), the triatomic molecule of water (H_2O) has a nonlinear structure: the respective distances between the atoms of oxygen and hydrogen and between the two hydrogen atoms are $\bar{d}_{OH} \approx 9.57\ 10^{-11}$ m and $\bar{d}_{HH} \approx 1.54\ 10^{-10}$ m (see also Figure 2.4a). These distances are the ones prevailing in the equilibrium state, when the angle HOH $\bar{\alpha}_{HOH} \approx 104.5^{\circ}$. These parameters define the geometry of the water molecule, in which a rotation through an angle π or 2π around the axis of rotation in the planes

TABLE 2.1. Selected physical properties of the water molecule $^1H_2{}^{16}O$, governing its interaction with electromagnetic radiation or associated with its optical properties.

No.	Name or symbol (explanation)	Value: In common units	Value: In SI units
-1-	*-2-*	*-3-*	*-4-*
	Geometrical Parameters		
1	Mean OH bond length in the ground state $\bar{d}_{OH}$	0.9572 (±0.0003) Å	9.572 (±0.003) × 10^{-11}m
2	Mean HOH bond angle in the ground state $\bar{\alpha}_{HOH}$	104.52° (± 0.05°)	1.82 rad (± 8.43×10^{-4} rad)
3	Mean distance between H atoms in the ground state $\bar{d}_{HH}$	c. 1.54 Å	c. 1.54×10^{-10} m
	Dynamic Parameters		
4	Inert molecular weight m_{H_2O}	$2.9907243 \times 10^{-23}$ g	$2.9907243 \times 10^{-26}$ kg
5	Moments of inertia in the ground state(*): $I^y_{H_2O}$	2.9376×10^{-40} g cm^{-2}	2.9376×10^{-39} kg m^{-2}
6	$I^z_{H_2O}$	1.959×10^{-40} g cm^{-2}	1.959×10^{-39} kg m^{-2}
7	$I^x_{H_2O}$	1.0220×10^{-40} g cm^{-2}	1.0220×10^{-39} kg m^{-2}
	Electric and Magnetic Properties		
8	Relative permittivity (dielectric constants) ε	Gas: 1.0059 (100°C, 101.325 kPa) Liquid: 87.9 (0°C), 78.4 (25°C), 55.6 (100°C) Ice Ih: 99 (–20°C), 171 (–120°C)	
9	Relative polarizability α/ε_0 (where α = polarizability, ε_0 = permittivity of a vacuum)	1.44×10^{-10} m^3	
10	Dipole moment in the equilibrium state p_p	Gas: 1.854 D (debye) Liquid (27°C): 2.95 D Ice Ih: 3.09 D	6.18×10^{-30} A s m 9.84×10^{-30} A s m 10.31×10^{-30} A s m
11	Volume magnetic susceptibility $\chi = \mu - 1$ (where μ - relative magnetic permeability) at 20 °C	-7.19×10^{-7} [dimensionless] (cgs convention)	-9.04×10^{-6} [dimensionless]

TABLE 2.1. Selected physical properties of the water molecule $^{1}H_{2}{}^{16}O$, governing its interaction with electromagnetic radiation or associated with its optical properties.—Cont'd.

No.	Name or symbol (explanation)	Value	
		In common units	In SI units
-1-	*-2-*	*-3-*	*-4-*
	Characteristic Molecular Energies		
12	Bond energy between the constituent atoms in the molecule at temperature 0K	−9.511 eV	-1.52×10^{-18} J
12a	As above, at temperature 25°C	−10.09 eV	-1.62×10^{-18} J
13	Ground state vibrational energy	+0.574 eV	9.20×10^{-20} J
14	Energy of electronic bonds (the difference (12) – (13))	−10.085 eV	-1.62×10^{-18} J
15	The sum of the energies of the discrete constituent atoms in the ground state	−2070.46 eV	-3.32×10^{-16} J
16	The total energy of the molecule at temperature 0 K (sum of (14) + (15))	−2080.55 eV	-3.33×10^{-16} J
16a	The kinetic energy input (equal to-(16))	+2080.55 eV	3.35×10^{-16} J
16b	The potential energy input (equal to 2(16) – (17))	−4411.3 eV	-7.07×10^{-16} J
17	Nuclear repulsion energy	+250.2 eV	4.01×10^{-17} J
18	Electronic excitation energy at light wavelength $\lambda = 124$ nm	c. 10.0 eV	c. 1.60×10^{-18} J
19	Ionization potential first (I)	12.62 eV	2.02×10^{-18} J
20	Second (II)	14.73 eV	2.36×10^{-18}
21	Third (III)	16.2 ±0.3 eV	2.60×10^{-18} J $\pm 4.81 \times 10^{-20}$ J
22	Fourth (IV)	18.0 ± 0.3 eV	2.88×10^{-18} J $\pm 4.81 \times 10^{-20}$ J
23	Total H–O bond energy at temperature 0K (equal to 1/2 (12))	−4.756 eV	-7.62×10^{-19} J
24	Dissociation energy of H–O bond at temperature 0 K	4.40 eV	7.05×10^{-19} J
25	Dissociation energy of H–OH bond at temperature 0 K (equal to-(12) – (24))	5.11 eV	8.19×10^{-19} J
26	Energy of the lowest vibrational transition	0.198 eV	3.17×10^{-20} J
27	Typical energy of a rotational transition	0.005 eV	8.01×10^{-22} J
28	Change of internal energy per molecule during the formation of water vapor at boiling point	0.39 eV	6.25×10^{-20} J
29	Change of internal energy per molecule during the formation of type Ih ice at temperature 0°C	−0.06 eV	-9.61×10^{-21} J
30	Change of internal energy per molecule during the transition from type Ih ice to type II ice	−0.0007 eV	-1.12×10^{-22} J

(*Continued*)

TABLE 2.1. Selected physical properties of the water molecule $^{1}H_{2}{}^{16}O$, governing its interaction with electromagnetic radiation or associated with its optical properties.—Cont'd.

No.	Name or symbol (explanation)	Value	
		In common units	In SI units
-1-	*-2-*	*-3-*	*-4-*
	$^{1}H_{2}{}^{16}O$ Occurrence on the Background of Molar Isotopic Composition of Natural Waters (according to VSMOW[a])		
		Percent of total mass	
31	$H_{2}{}^{16}O$	99.7317	
32	$H_{2}{}^{17}O$	0.0372	
33	$H_{2}{}^{18}O$	0.199983	
34	$HD^{16}O$	0.031069	
35	$HD^{17}O$	0.0000116	
36	$HD^{18}O$	0.0000623	
37	$D_{2}{}^{16}O$	0.0000026	
38	$HT^{16}O$	variable trace	
39	$T_{2}{}^{16}O$	~ 0	

After various authors, cited in Eisenberg and Kauzman (1969), Haken and Wolf (1995,1998), Dera (2003), and Chaplin (2006); among others.

* Moment of inertia: (y) = relative to the *y*-axis passing through the center of mass of the molecule and perpendicular to the HOH plane; (z) = relative to the axis bisecting the angle α_{HOH}; (x) = relative to the axis perpendicular to the (y,z) plane and passing through the center of mass.

[a] The Vienna Standard Mean Ocean Water (VSMOW) for a general number of hydrogen atoms contains 99.984426% atoms of ^{1}H, 0.015574% atoms of ^{2}H (D), and 18.5×10^{-16}% atoms of ^{3}H (T), and for a general number of oxygen atoms contains 99.76206% atoms of ^{16}O, 0.03790% atoms of ^{17}O and 0.20004% atoms of ^{18}O (see, e.g., Chaplin (2006)).

of symmetry (the plane of the molecule, and the plane perpendicular to it, passing through the oxygen atom) do not affect its configuration. Determined with respect to these axes of rotation, the three moments of inertia of the water molecule are different (see items (5)–(7) in Table 2.1). It is for these reasons that we replace the description of the rotational motion of the water molecule by a quantum description of the motion of an asymmetrical top. This approach makes it very much easier to describe the purely rotational spectrum of the vibrations of the water molecule.

The asymmetrical structure of the water molecule, which can be likened to a three-dimensional anharmonic vibrator, also affects its vibrational states. It is responsible for the fact that water molecules have a high, permanent dipole moment: $p_p = 1.854$ debye in the equilibrium state (see item (10) in Table 2.1). The value of this dipole moment changes due to the interaction of interatomic forces, which alter the individual interatomic distances in the molecule and also the angle α_{HOH} between the OH bonds. The effect of these interactions manifests itself as vibrations of the atoms around their equilibrium positions in the molecule's electric field; generally characteristic of a particular molecule, this effect depends on its structure. The number f of normal vibrations of a molecule depends on the number of its internal degrees of freedom N:

$$f = 3N–5 \text{ for linear molecules.}$$

$$f = 3N–6 \text{ for nonlinear molecules.}$$

In the water molecule ($N = 3$) there are thus three "modes" of normal vibrations, described by three vibrational quantum numbers: υ_1 (mode I), υ_2 (mode II), and υ_3 (mode III); see Figure 2.1. As this figure shows, the vibrational modes characteristic of the water molecule differ. The excited vibrations of mode I are symmetric stretch vibrations, whereas those of mode II are deformation vibrations, causing the molecule to bend. Mode III vibrations are asymmetric stretch vibrations.

We describe the vibrational energy states of the water molecule by stating the values of all three of its vibrational quantum numbers: υ_1, υ_2, and υ_3. In the ground (not excited) vibrational state the values of all three quantum numbers are zero, so that we can write this state as (0,0,0). The vibrational

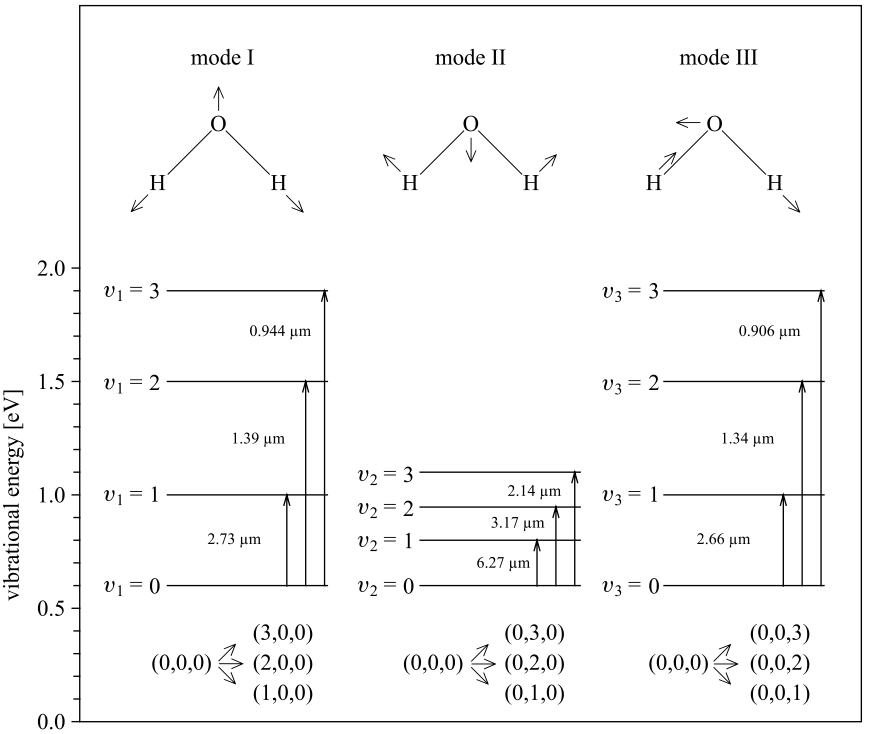

FIGURE 2.1. Normal vibration modes of a water molecule and its characteristic vibrational energy levels in the ground state, and in selected vibrational excited states described by quantum numbers υ_1, υ_2, and υ_3. The figure also gives the approximate wavelengths of light [μm] absorbed by such a molecule during its transition from the ground state to these excited states. The exact values of the vibrational energies shown in the figure are given in Table 2.2.

TABLE 2.2. Vibrational energies of the water molecule E_{VIB} in the ground state and selected simple excited states.[a]

Quantum number υ_1 or υ_2 or υ_3	Mode I (υ_1) E_{VIB} [eV]	Mode II (υ_2) E_{VIB} [eV]	Mode III (υ_3) E_{VIB} [eV]
-1-	*-2-*	*-3-*	*-4-*
0	0.574	0.574	0.574
1	1.03	0.772	1.04
2	1.47	0.965	1.5
3	1.89	1.15	1.94
4	2.34	1.33	2.38
5	2.74	1.51	2.80
6	3.12	1.67	3.21
7	3.55	1.83	3.61

Calculated from data in Eisenberg and Kauzmann (1969) and Lemus (2004).
[a] That is, for the vibrations of one mode.

energy of the water molecule in this state is $E_{VIB} = 0.574$ eV (i.e., 9.20×10^{-20} J). In the excited states of the molecule, its vibrational energy is greater, every higher level of excitation being described by the corresponding higher value of the vibrational quantum number. This is exemplified in Table 2.2, which gives the vibrational energies of the water molecule in various "simple" excited states, that is, when it is vibrating in only one of its modes. The data in Table 2.2 show that these energies vary for different modes. The most highly energetic ones are the asymmetric stretch vibrations, that is, mode III. Only slightly less energetic are the symmetric stretch vibrations (mode I). Finally, the vibrations with the lowest energy (less than the previous two types by c. 30–60%, depending on the level of excitation) are the mode II deformation vibrations. These differences exert a fundamental influence on the position of the light absorption spectral bands associated with the molecule's different vibrational modes (see below), these bands arising as a result of transitions between lower and higher vibrational-rotational energy levels. These transitions can be divided into a number of groups, which we now briefly discuss.

Fundamental Transitions

Transitions from the ground state to the first excited state in a given mode are recorded in the light absorption spectrum as fundamental absorption bands, which can be written as follows:

$$(0,0,0) \rightarrow (1,0,0) \text{ mode I}$$

$$(0,0,0) \rightarrow (0,1,0) \text{ mode II}$$

$$(0,0,0) \rightarrow (0,0,1) \text{ mode III}$$

If we know the vibrational energy of the ground state E_{VIB1} and the energies of the first excited state E_{VIB2} for each of the three vibrational modes (see Table 2.2), we can easily work out the positions in the spectrum of these three

fundamental absorption bands for the water molecule from the differences between these energies.[1] In the spectrum, the fundamental light absorption bands for the vibrational modes I, II, and III of the water molecule lie in the vicinity of the wavelengths λ = 2.73 μm, 6.27 μm, and 2.66 μm, respectively. As we can see, all three bands lie in the IR region, whereby the longest-wave band (i.e., with the lowest energy of absorbed photons) is due to mode II vibrations. In contrast, the changes in the energy states of the water molecule performing mode I or mode III vibrations cause radiation of a much shorter wavelength, that is, much higher-energy photons to be absorbed (or emitted).

In addition to these three fundamental bands of light absorption or emission, corresponding to molecular transitions from the ground state to the first excited state, or back from the latter state to the former (i.e., transitions for which the condition $\Delta\upsilon_1 = \pm 1$, $\Delta\upsilon_2 = \pm 1$, or $\Delta\upsilon_3 = \pm 1$ is satisfied), the absorption spectrum of the water molecule reveals a whole series of further bands due to energy transitions between various vibrational levels. For analyzing their origin and characteristic features, it is convenient to distinguish four categories of such transitions, namely:

- Harmonic transitions (also known as overtones) from the ground state
- Combination transitions from the ground state
- Harmonic transitions between excited states only
- Combination transitions between excited states only

We now proceed to discuss the meanings of these concepts and the positions of the absorption bands to which they give rise.

Harmonic and Combination Transitions from the Ground State

In the water molecule, inasmuch as it is anharmonic, further transitions are allowed from the ground state to higher excited states in a given mode (i.e., as a result of which one of the three vibrational quantum numbers changes: $\Delta\upsilon_1$ or $\Delta\upsilon_2$ or $\Delta\upsilon_3 > 1$. As a consequence of these transitions, harmonic absorption bands are formed, also known as overtones. We can write these transitions as above, but with higher values of the quantum numbers υ'_1, υ'_2, υ'_3 = 2, 3, . . . ; for example, (0,0,0) → (0,2,0) denotes a mode II transition from the ground state to the first state of harmonic vibrations The quantum mechanical selection rules also allow transitions in the water molecule from the ground state to narrower vibrational energy states with a simultaneous change of more than one vibrational quantum number. An example of such a change is (0,0,0) → (3,1,1), which means that on absorbing a photon, the molecule passes from the ground state to an excited state that is a mixture of

[1] The wavelength of a photon absorbed (or emitted) by a molecule is given by the obvious relationship $\lambda = hc/(E_{VIB2} - E_{VIB1})$, derived from Equation (2.2), where E_{VIB1} is the ground state energy (i.e., (0,0,0); E_{VIB2} is the excited state energy (i.e., in this particular case (1,0,0), (0,1,0), or (0,0,1)).

all three vibrational modes, because all three quantum numbers have changed by $\Delta\upsilon_1 = 3$, $\Delta\upsilon_2 = 1$, $\Delta\upsilon_3 = 1$. Transitions of this type give rise to so-called combination absorption bands.

There may be a large number of such harmonic and combination absorption bands. In practice we find several tens of them in any spectrum (Eisenberg and Kauzmann 1969, Lemus 2004). The more important of these bands, recorded experimentally, are listed in Table 2.3 together with the definition of

TABLE 2.3. Vibrational bands of light absorption by H_2O molecules excited from the ground state.

Quantum numbers of excited states υ_1, υ_2, υ_3	Wavelength [μm]	Quantum numbers of excited states υ_1, υ_2, υ_3	Wavelength [μm]
-1-	*-2-*	*-1-*	*-2-*
0,1,0	6.27	1,2,2	0.733
0,2,0	3.17	2,2,1	0.732
1,0,0	2.73	1,7,0	0.732
0,0,1	2.66	2,0,2	0.723
0,3,0	2.14	3,0,1	0.723
1,1,0	1.91	0,7,1	0.723
0,1,1	1.88	1,2,2	0.719
0,4,0	1.63	0,2,3	0.711
1,2,0	1.48	4,0,0	0.703
0,2,1	1.46	1,0,3	0.698
2,0,0	1.39	0,0,4	0.688
1,0,1	1.38	1,5,1	0.683
0,0,2	1.34	1,3,2	0.662
0,5,0	1.33	2,3,1	0.661
1,3,0	1.21	2,1,2	0.652
0,3,1	1.19	3,1,1	0.652
2,1,0	1.14	0,3,3	0.644
1,1,1	1.14	4,1,0	0.635
0,6,0	1.13	1,1,3	0.632
0,1,2	1.11	3,2,1	0.594
0,4,1	1.02	2,2,2	0.594
2,2,0	0.972	3,0,2	0.592
1,2,1	0.968	2,0,3	0.592
0,2,2	0.950	4,2,0	0.580
3,0,0	0.944	1,2,3	0.578
2,0,1	0.942	5,0,0	0.573
1,0,2	0.920	4,0,1	0.572
0,0,3	0.906	1,0,4	0.563
1,3,1	0.847	3,3,1	0.547
1,1,2	0.824	3,1,2	0.544
2,1,1	0.823	2,1,3	0.544
1,1,2	0.806	4,1,1	0.527
0,1,3	0.796	3,0,3	0.506
2,4,0	0.757	5,0,1	0.487
1,4,1	0.754	3,1,3	0.471
0,4,2	0.744	4,0,3	0.444

Based on data gleaned from Lemus (2004).

the type of transition. We should bear in mind, however, that the intensities of the spectral lines in bands corresponding to harmonic vibrations and also in combination bands, are several orders of magnitude less than the intensities of the fundamental lines.

As we can see from Table 2.3, these harmonic and combination absorption bands of the water molecule lie in the near-infrared region of the spectrum, and some of them encroach into the visible region. This means that such photons are absorbed in the transitions, whose energies exceed those of the photons absorbed during fundamental transitions. Absorption of these photons is reflected in the spectrum by the fundamental absorption bands in the vicinity of wavelengths 2.73 μm (mode I), 6.27 μm (mode II), and 2.66 μm (mode III). These last wavelengths, characteristic of the fundamental bands of light absorption by the water molecule, constitute the longwave boundaries (at the longwave end of the spectrum) of the sets of wavelengths corresponding to all the possible absorption bands due to molecular transitions from the ground state to diverse excited states.

On the other hand, at the shortwave end, there is no such boundary due to vibrational transitions. Theoretically, however, we could expect there to be, in this region of the spectrum, shortwave boundaries connected with molecular dissociation, separating the several vibrational-rotational absorption spectra from the continuum absorption spectrum. These boundaries are delineated by the wavelengths of photons, whose absorption (associated with the transition from the ground vibrational state to an excited state with quantum numbers taking infinitely large values) causes the water molecule to dissociate, or more precisely, causes first the H–OH bond, then the H–O bond, to break down (see Table 2.1, items 24 and 25). These are waves of length c. 0.28 μm breaking the H–O bond (dissociation energy c. 4.4 eV) and c. 0.24 μm for the H–OH bond (dissociation energy c. 5.11 eV). On the longwave side of these boundaries the absorption spectrum should consist of separate bands, corresponding to the excitation of successively higher vibrational states. On the shortwave side, however, it should be a continuum, inasmuch as there can be no question of any quantized, discrete energy levels being present in such a configuration. Quite simply, the excess energy of the absorbed photon, beyond that required to dissociate a molecule, may be converted into the kinetic energy (of any value) of these dissociated fragments of the molecule.

Theoretically, therefore, we can also expect there to be vibrational-rotational absorption bands due to transitions of the water molecule to very high vibrational energy states, lying not only in the visible region of electromagnetic waves, but also in the ultraviolet. Empirically, however, such absorption bands are not recorded for water. This is very likely because they are of very low intensity, because the probability of energy transitions of the molecule decreases sharply as the energy of the photons increases. Direct photodissociation of the water molecule only by vibrational-rotational excitation, in the absence of electronic excitation, is so very unlikely as to be practically impossible. Being a single-photon process, it is forbidden by the

selection rules for vibrational transitions, which only allow transitions involving a small change in the vibrational quantum numbers. It is also forbidden by the Franck–Condon principle (see, e.g., Barrow (1969) and Haken and Wolf (1995)). Photodissociation is, however, possible as a result of the absorption of high-energy photons, which give rise to transitions between the electronic energy states of the molecule. We return to the problem of photodissociation in Section 2.1.2.

Harmonic and Combination Transitions Between Excited States

Apart from the aforementioned fundamental vibrational transitions and their overtones and combination transitions from the ground state, whose absorption bands lie in the near-IR and visible regions of the spectrum—$\lambda \leq 6.27$ μm (i.e., the fundamental band of mode II)—the water molecule can, as a result of vibrational transitions, also absorb radiation of a longer wavelength, in the region of $\lambda > 6.27$ μm. The differences in vibrational energy between successive, ever higher vibrational states diminish with the increasing quantum numbers characterizing these states (see, for instance, the successive vibrational energies given in Table 2.2). Therefore, if vibrational transitions, both harmonic and combination, are going to take place solely between excited states, they can be induced not only by photons with energies higher (shorter wavelengths) than those required for transitions from the ground state (because the quantum numbers of ground states are sufficiently low and those of the final states sufficiently high), but also by lower-energy photons (i.e., longer wavelengths;[2] because the quantum numbers of the initial and final states are sufficiently high and the differences $\Delta\upsilon$ sufficiently low).

In practice, however, transitions between excited states are far less probable than fundamental transitions or overtones and combination transitions from the ground state. Hence, the absorption bands due to transitions between excited states are far less intense. This is because under normal illumination conditions (e.g., when the sea is illuminated by daylight) the number of molecules not excited (or in very low states of excitation) far exceeds the number of highly excited molecules. So the probability of "coming across" (and absorbing a photon from) a highly excited molecule is many orders of magnitude lower than that of coming across (and absorbing a photon from) a molecule in the ground or a low excited state.

Transitions Between the Vibrational States of Different Isotopes of Water

We should also mention that in natural aquatic environments, or other environments containing water in different states of aggregation, in addition to the

[2] For example, the following simple transitions for the case of mode II: (0,1,0) → (0,2,0), and (0,2,0) → (0,3,0), and so on, are due to the absorption of photons of 6.42 μm, 6.57 μm, and so on, that is, of a longer wavelength than the fundamental band at 6.27 μm.

TABLE 2.4. Positions of light absorption bands of isotopic variants of water molecules on excitation from the ground state.

Quantum numbers of excited states	Wavelength λ [μm]					
$\upsilon_1, \upsilon_2, \upsilon_3$	$H_2{}^{16}O$	$H_2{}^{17}O$	$H_2{}^{18}O$	$HD^{16}O$	$D_2{}^{16}O$	$T_2{}^{16}O$
-1-	*-2-*	*-3-*	*-4-*	*-5-*	*-6-*	*-7-*
0,1,0	6.27	6.28	6.30	7.13	8.49	10.05
1,0,0	2.73	2.74	2.74	3.67	3.47	4.48
0,0,1	2.66	2.67	2.67	2.70	3.59	4.23
0,2,0	3.17	—	—	3.59	—	—
0,1,1	1.88	—	—	1.96	2.53	—
0,2,1	1.45	—	—	1.55	1.96	—
1,0,1	1.38	—	—	1.56	1.86	—
1,1,1	1.28	—	—	—	1.53	—
2,0,1	0.942	—	—	—	1.27	—

Based on data from: Eisenberg and Kauzmann (1969) and Chaplin (2006) (http://www.lsbu.ac.uk/water/vibrat.html).

overwhelming numbers of water molecules H_2O consisting of the most common isotopes of hydrogen and oxygen (^1H, ^{16}O), there are, although in very much smaller quantities, also water molecules made up of the heavier isotopes of hydrogen and oxygen (e.g., $^1H_2{}^{17}O$; $^1H_2{}^{18}O$; $^1H^2D^{16}O$; $^2D_2{}^{16}O$; $^3T_2{}^{16}O$). It turns out that the parameters of such molecules differ dynamically from those of ordinary water $^1H_2{}^{16}O$. Consequently, the excited state vibrational energies of these heavier variants of water are generally lower. This quite substantially increases the length of the light waves emitted or absorbed as a result of transitions between their vibrational states. Examples of such transitions can be found in Table 2.4.

A Simple Analytical Description of the Vibrational States of the Water Molecule

An exact definition of the vibrational energies of the various possible states of the molecule, and hence the parameters (energy, wave number, wavelength) of the photons absorbed or emitted as a result of changes in these states, demands time-consuming model quantum-mechanical calculations,[3] or else complex experimental procedures. As Benedict et al. (1956) demonstrated (see also Eisenberg and Kauzmann (1969)), however, there is a straightforward empirical formula for water and its isotopic variants, which describes with good accuracy these vibrational energies in the ground state and in a

[3] An example of such calculations of arbitrary vibrational states of the $H_2{}^{16}O$ molecule are those by Lemus (2004) using a model he derived himself. In his work he gives a vibrational description of $H_2{}^{16}O$ in terms of Morse local oscillators for both bending and stretching degrees of freedom.

whole range of excited states. This applies to simple excited states (when only one mode of vibration is excited), and also to mixed states (when various arbitrary configurations of two or all three modes are excited) with low or medium states of excitation, such as may occur under natural conditions. This formula makes the vibrational energy of a water molecule E_{VIB} dependent on the quantum numbers $\upsilon_1\ \upsilon_2\ \upsilon_3$ and takes the form:

$$E_{VIB}(\upsilon_1,\upsilon_2,\upsilon_3) = hc\left[\sum_{i=1}^{3}\omega_i\left(\upsilon_1+\frac{1}{2}\right) + \sum_{i=1}^{3}\sum_{k\geq i}^{3}x_{i,k}\left(\upsilon_i+\frac{1}{2}\right)\left(\upsilon_k+\frac{1}{2}\right)\right], \tag{2.3}$$

where: h is Planck's constant; c is the velocity of light in a vacuum; i is the number of the vibrational mode; k is a natural number taking values from i to 3; and ω_i [cm^{-1}] and $x_{i,k}$ [cm^{-1}] are empirical constants whose values for the water molecule and selected variants of it are given in Table 2.5.

The terms ω_i appearing in expression (2.1.3) have the dimension [cm^{-1}] and describe the component frequencies (more precisely, the wave numbers) of the harmonic vibrations of the bonds in the water molecule, whereas the terms $x_{i,k}$ (expressed in [cm^{-1}]) are anharmonic constants describing the effect (on the resultant frequency of vibrations) of deviations of a real anharmonic vibrator from the oscillations of a harmonic vibrator. The above formula may be very useful in practice, as it allows us to define simply the energies of the various possible vibrational states of the water molecule, and hence, also the energies, frequencies, and wavelengths of the photons absorbed or emitted during transitions of the molecule between these states.

TABLE 2.5. Values of the constants appearing in Equation (2.3) describing the vibrational state energies of water molecules H_2O, D_2O, and HDO.

Molecule	Constant harmonic and anharmonic frequencies [cm^{-1}]								
	ω_1	ω_2	ω_3	x_{11}	x_{22}	x_{33}	x_{12}	x_{13}	x_{23}
-1-	*-2-*	*-3-*	*-4-*	*-5-*	*-6-*	*-7-*	*-8-*	*-9-*	*-10-*
H_2O	3832.17	1648.47	3942.53	–42.576	–16.813	–47.566	–15.933	–165.824	–20.332
HDO	2824.32	1440.21	3889.84	–43.36	–11.77	–82.88	–8.60	–13.14	–20.08
D_2O	2763.80	1206.39	2888.78	–22.58	–9.18	–26.15	–7.58	–87.15	–10.61

Based on Benedict et al. (1956).

Rotational Transitions

Because molecular rotations are not a factor that noticeably affects the resultant absorption spectra of liquid water in the sea, we deal with this particular problem here rather briefly.

As we said at the beginning of this section, transitions between the various vibration states of a molecule are accompanied by changes in its rotational

states. If we use a spectrophotometer with sufficient resolving power to record IR absorption spectra of molecules in the gas state (i.e., separate molecules), we shall see that these spectra are not smooth, but take the form of bands with an extremely intricate structure. Resulting from changes in the rotational states of molecules, these bands appear both on the longwave side of the central line corresponding to a purely vibrational transition, that is, when the rotational energy decreases (the P($\Delta J = -1$) branch), and also on the shortwave side of this line, that is, when the rotational energy increases following the absorption of these waves (the R($\Delta J = +1$) branch). It is often the case that the lines of these bands are even more intense than the central line, corresponding to a purely vibrational transition, with no change in the rotational energy (band Q ($\Delta J = 0$). Figure 2.2 illustrates such examples for water vapor in the atmosphere. In condensed phases (liquid water, ice), however, where the molecules are acted upon by the forces of their interaction, the rotational energy levels are subject to line broadening. Hence in liquid water, the rotational structure in vibrational absorption bands is scarcely visible, if at all.

The limiting cases of transitions between the vibrational-rotational energy states of molecules are those where the vibrational quantum numbers do not change; only the rotational states of the molecules do so. Then we have a purely rotational transition. Because the fundamental rotational energies of molecules are usually c. 100 times smaller than their vibrational energies, such rotational transitions involve the absorption or emission of low-energy

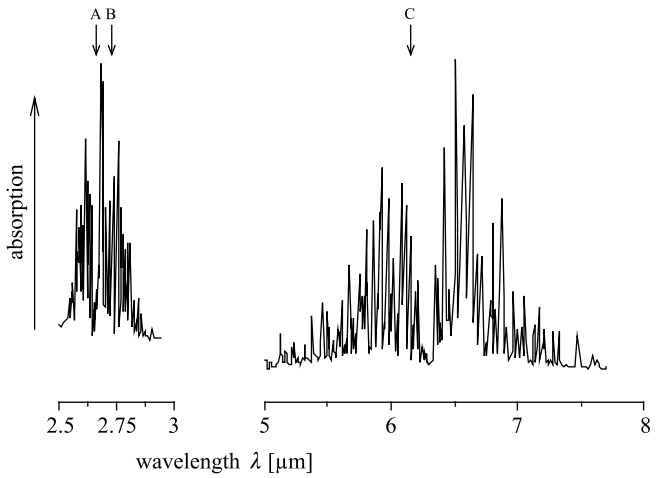

FIGURE 2.2. Absorption spectrum of water vapor corresponding to the three principal vibrational transitions and showing part of the rotational structure: A, 2.66 μm band, corresponding to mode III, that is, (0,0,0) → (0,0,1); B, 2.73 μm band, corresponding to mode I, that is, (0,0,0) → (1,0,0); C, 6.27 μm band, corresponding to mode II, that is, (0,0,0) → (0,1,0). (Adapted from Banwell (1985).)

radiation. The photon energies required to induce such transitions in water molecules are of the order of $10^{-2} - 10^{-3}$ eV, (i.e., light in the far IR). Hence, the rotational bands of light absorption for these molecules lie in the far infrared, microwave, and radiowave regions of the spectrum. The most intense absorption lines of these bonds appear in the 50 μm region (Eisenberg and Kauzmann 1969). Also characteristic are the absorption bands of quanta of wavelengths 27.9 μm and 118.6 μm, and in the vicinity of 1.64 mm and 1.35 cm (Shifrin 1983b, 1988).

Vibrational-Rotational Absorption Spectra of the Water Molecule

The large number of vibrational-rotational energy transitions in the water molecule allowed by the quantum-mechanical selection rules means that the light absorption spectrum of this molecule over the whole wavelength range of IR and microwaves is an extremely complex one, consisting of many bands of different intensities and widths. This is exemplified in Figure 2.3 by the spectrum of the specific light absorption coefficient of water vapor in the atmosphere, which we defined approximately[4] on the basis of empirical data and information gleaned from the works of the various authors cited in the caption to this figure. The absorption of radiation in rarefied water vapor is practically of the same nature as absorption by discrete molecules of water.

As we can see in Figure 2.3, the most intense bands in the near-IR region are the three fundamental absorption bands corresponding to vibrational-rotational transitions of the water molecule from the ground state to the first excited state in the relevant vibrational mode (see the band marked X and 6.3μ). The most intense and the widest of these three bands is the one corresponding to vibrational-rotational transitions in vibrational mode II, deforming the molecules. The center of this band lies around the wavelength $\lambda = 6.27$ μm. This band possesses a fine structure (not visible on the spectrum), in which there appear a large number of spectral lines varying in width and intensity. These lines, including the weakest ones in this intense band, can be identified in the Earth's atmosphere, even in the so-called "windows" in the absorption spectrum of the atmosphere (Kondratev 1969).

---

[4] Owing to the fine structure of the absorption bands of gases in the IR, which consist of narrow, almost monochromatic, natural absorption lines and narrow "absorptionless intervals" between them, the exact empirical determination of the so-called "logarithmic" coefficients of absorption (the ones applied inter alia in marine optics) is complicated and can be achieved only to a greater or lesser approximation. This is because the widths of these natural absorption lines and "absorption less intervals" in the absorption spectrum are usually much smaller than those of the spectral detection intervals, which are a consequence of the resolving powers of spectrophotometers. With respect to water vapor, these questions are discussed by Kondratev (1969) and Bird and Riordan (1986), among others.

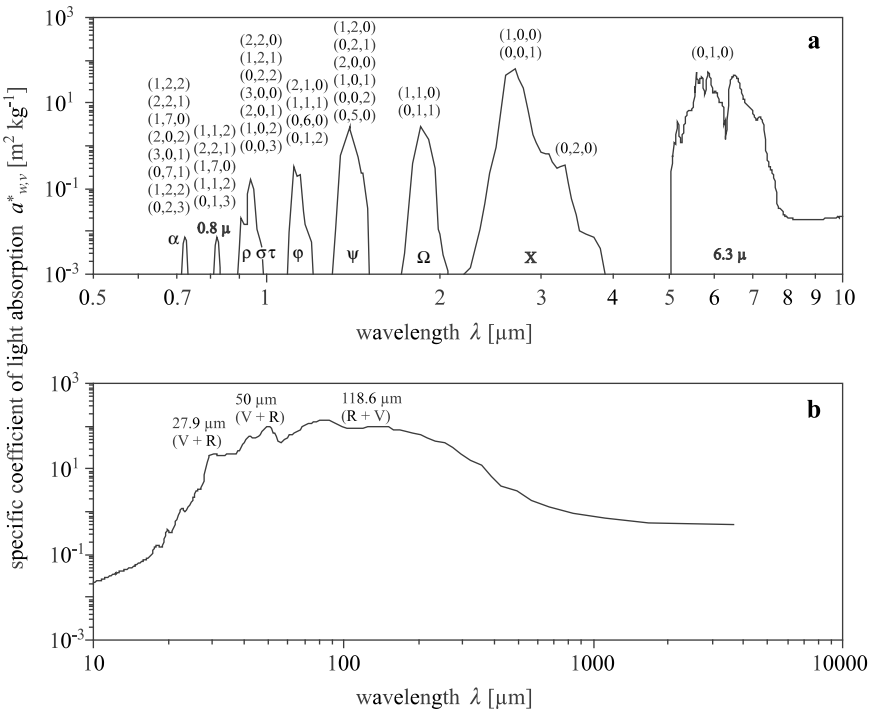

FIGURE 2.3. Spectrum of the approximate specific coefficient of IR and microwave absorption for atmospheric water vapor $a^*_{w,v}$; the details of the rotational structures (as visible on Figure 2.2) have been omitted. (a) standard (atmospheric optical) codes for the various bands are given below the plot; the excitations responsible for absorption (from the ground state) of the various vibrational states (υ_1, υ_2, υ_3) are stated in parentheses above the relevant bands; (b) (V + R) denotes the absorption peaks due to the overlapping of vibrational-rotational and rotational bands; (R + V) denotes the peaks due mainly to rotational transitions. This spectrum was plotted on the basis of empirical data and other information taken from Yamamoto and Onishi (1952), Shifrin (1983b, 1988), Kondratev (1969), Bird and Riordan (1986).

Somewhat less intense and narrower than the previous band is the fundamental absorption band formed as a result of vibrational-rotational transitions in mode III of the water molecule. The center of this band lies in the vicinity of wavelength $\lambda = 2.66$ μm. Near this band we find the fundamental absorption band of the water molecule in the vicinity of $\lambda = 2.73$ μm, corresponding to vibrational-rotational transitions in mode I. These last two bands ((0,0,1) and (1,0,0)), and the harmonic band (0,2,0) in the vicinity of $\lambda = 3.17$ μm, partially overlap, together forming one very wide absorption band of the water molecule in the wavelength range from $\lambda = 2.3$ μm to $\lambda = 3.9$ μm (marked X on the spectrum). This band as a whole is the most

characteristic one of the water molecule and plays an important part in Nature in the absorption of near-IR radiation (Hollas 1992).

In the near-IR the water molecule also absorbs radiation of wavelengths $\lambda \approx 0.81$ μm, $\lambda \approx 0.94$ μm, $\lambda \approx 1.13$ μm, $\lambda \approx 1.38$ μm, and $\lambda \approx 1.88$ μm (see the bands denoted by the symbols 0.8μ, ρστ, φ, Ψ, and Ω in Figure 2.3a). The absorption of energy quanta of these wavelengths involves energy transitions of the water molecule, in which, according to the selection rules, the values of at least two vibrational quantum numbers change simultaneously (e.g., the band for $\lambda = 1.88$ μm is associated mainly with the transition (0,0,0) → (0,1,1). The widths and intensities of these last absorption bands vary, but they are many times smaller than the three fundamental bands we discussed earlier. Close by this last-mentioned group of bands we find narrow, low-intensity absorption bands corresponding to higher harmonic vibrations of the water molecule (overtones) as well as further allowed combination bands, that is, a combination of the aforementioned vibrational modes of the water molecule and their higher harmonics. Meriting our particular attention are those combination bands lying in the visible part of the spectrum ($\lambda < 0.8$ μm). They form a single, quite strong absorption band in the atmosphere, denoted on the spectrum by the symbol α, with an absorption maximum at $\lambda \approx 718$ nm. This is the only clear visible band of light absorption by the water molecule in the visible range of electromagnetic waves.

We now move on to the absorption of light in the somewhat farther infrared (see Figure 2.3b). Here we find the slight absorption by the water molecule of energy quanta from the wavelength range $12 < \lambda < 20$ μm, which corresponds to higher harmonic vibrations in modes I and II, and is characteristically very variable in intensity, this increasing with the wavelength of the absorbed light in this spectral region. In the wavelength range 20 μm $< \lambda <$ 1 mm the absorption spectrum is practically a continuum, but a few bands of greater intensity, among them, of wavelengths $\lambda = 27.9$ μm, $\lambda = 50$ μm, and $\lambda = 118.6$ μm, do stand out. The continuum absorption spectrum of the water molecule in this range is due to the superposition of vibrational-rotational bands with the spectral lines induced by purely rotational energy transitions. Nevertheless, the two strongest microwave absorption bands due to rotational transitions in the water molecule lie in the vicinity of the wavelengths $\lambda = 1.64$ mm and $\lambda = 13.48$ mm (Shifrin 1983b, 1988) (these last are not shown in Figure 2.3b).

2.1.2 Electronic Absorption Spectra

Molecules can absorb or emit radiation not only as a result of changes in their rotational and vibrational energies, as we have just been discussing, but also in consequence of changes in their electronic configurations, and hence, their electronic energy. Energy changes caused by a transition from one electronic state to another are usually quite large, corresponding to the energies of photons in the ultraviolet region, and in the case of the large unsaturated

molecules, in the visible region as well. We discuss the formation of absorption spectra of such large molecules in Chapter 3; for the present, we focus our attention on the electronic spectra of the water molecule.

We should expect—as we stated at the beginning of this chapter—that alongside electronic transitions involving such large changes in energy, there would be changes in vibrational energy (much smaller) and changes in rotational energy (even smaller). Indeed, the example of water shows us that electronic transitions do in fact lead to the formation, not of single absorption or emission lines, but of entire complexes of electron-vibrational absorption and emission bands with a highly intricate fine structure.

The energies of the electronic states of a molecule depend on its electronic structure as determined by the electronic structure of its constituent atoms. In order better to illustrate this problem, we now introduce the concepts of atomic orbitals (AO) and molecular orbitals (MO). These orbitals are useful in defining the energy of individual electrons in atoms and molecules. Again, the changes in these electronic energies, specified by the quantum rules of selection, determine the energies of photons absorbed or emitted by given molecules; in other words, they determine which wavelengths of electromagnetic radiation will correspond to the photon energies of the transitions.

The Concept of an Orbital

The quantum-mechanical magnitude characterizing the state of an electron in an atom or molecule is the single-electron wave function $\varphi_e(x,y,z,s)$, called the spin orbital. For the sake of simplicity, we can represent it as the product of the configurational function $\psi_e(x,y,z)$, dependent only on the coordinates (symbols: x, y, z) of its position in space, and the spin (symbol s) function $\xi(s)$, dependent only on the electron's spin s:

$$\varphi_e(x,y,z,s) = \psi_e(x,y,z) \cdot \xi(s). \tag{2.4}$$

The configurational wave function $\psi_e(x,y,z)$ can be determined for any electron in an atom or molecule by assuming the "single-electron approximation" (discussed in greater detail in Section 3.1) and solving the spinless Schrödinger equation.[5] The energy of an electron at every point in space is proportional to $|\psi_e|^2$ and defines the spatial distribution of the electronic charge. For a better picture of the localization of an electron, it is convenient to use the concept of orbitals: AO when we are dealing with the electrons in an atom, and MO if the electrons are those in a molecule. We usually assume an orbital to be that volume of space in which the majority (e.g., 95%) of the electronic charge is concentrated, or to put it another way, that there is a 95% probability

[5] For complex molecules these solutions can be exceedingly time-consuming, which is why we often use suitable approximate methods, some of which are mentioned in due course.

of finding the electron in this space. Orbitals conceived in this way have various shapes and sizes and localizations within the confines of the atom or molecule, depending on the type of atoms or molecular bonds and on the configuration of electrons. In Chapter 3, we discuss many such electronic orbitals typical of atoms and complex molecules, that is to say, the many and diverse configurations of electrons in atoms and molecules absorbing light. Here we begin by presenting first the atomic orbitals of hydrogen and oxygen, and then the orbitals of the water molecule formed from these atoms.

Atomic Orbitals of Hydrogen and Oxygen; Molecular Orbitals of Water

Before describing the electronic states of the water molecule, let us recall briefly the main features and conventions applied to the description of electronic states in atoms. For this we use atomic orbitals, whereby every such orbital is unequivocally defined by the values of the following quantum numbers, which can be zero or an integer.

1. Principal quantum number $n = 1, 2, 3, 4, \ldots$, which is at the same time the number of the orbit or electronic shell.
2. Orbital quantum number $l = 0, 1, 2, \ldots, (n - 1)$, whose increasing values are denoted by the letters s, p, d, ... It is the quantum number of the orbital angular momentum (OAM) of the electron that defines the scalar value of this angular momentum in accordance with the expression: OAM $= \sqrt{l(l+1)}\, h/2\pi$ (h is Planck's constant); to the various letters l are attributed subshells (suborbits) denoted successively by the letters s, p, d, ...
3. Magnetic quantum number $m = -l, -l + 1, \ldots, 0, \ldots, +l$, which defines the scalar values of the projections of this orbital angular momentum on to $(2l + 1)$ distinct directions, equal $mh/2\pi$.

However, the energy state of every electron in an atom is characterized unequivocally by four quantum numbers. The first three are the ones just mentioned, n, l, m, characterizing the type of orbital, whereas the fourth quantum number of an electron is its spin number, or simply spin, which can take one of two values: +1/2 or −1/2. This is in agreement with the Pauli exclusion principle in quantum mechanics, according to which each electron in an atom (and also in a molecule) must differ from all the other electrons in the value of at least one of the four quantum numbers describing its state. Likewise, each atomic (and also molecular) orbital may contain at most two electrons with different spins. Notice too, that the four quantum numbers (n, l, m, s) so defined unequivocally determine the value of the electronic energy (mentioned earlier) described by the quantum number Λ, which defines the absolute value of the projection of the orbital angular momentum on to the axis of the molecule.

In accordance with this convention, the electronic configurations of the hydrogen and oxygen atoms forming the water molecule in the ground state can be written as:

Hydrogen: $1s^1$;
Oxygen: $[1s^2]$, $2s^2$, $2p_x^2$, $2p_y^1$, $2p_z^1$.

So every configurational code begins with a number equal to the principal quantum number, that is, the number of the orbit. The letter in position two of the code denotes the subshell; that is, it defines the orbital quantum number ($l = 0$ for s, $l = 1$ for p). Information about the magnetic quantum number is also given here. In the case of the s subshell (i.e., $1s$ for hydrogen, and $1s$ and $2s$ for oxygen) there is no extra information, because in this case $l = 0$, and the magnetic quantum number takes the only possible value of $(2l + 1) = 1$. But in the case of the $2p$ subshell (i.e., for $l = 1$) for oxygen, there are $(2l + 1) = 3$ possibilities, represented by the relevant components of the projection: $2p_x(m = 0)$, $2p_y$ $(m = -1)$ and $2p_z(m = +1)$. Finally, the superscript on the right-hand side of the various orbital codes indicates the number of electrons in these subshells (at most equal to two electrons with different spins). Filled inner shells, that is, shells containing their full complement of electrons, are customarily enclosed in square brackets (see the first shell for oxygen, $[1s^2]$).

The approximate shapes and orientations in space of the atomic orbitals of hydrogen and oxygen are illustrated in Figure 2.4b,c. In the same figure (Figure 2.4d,e,f) there is a schematic representation of how the atomic orbitals of the valence electrons of the two hydrogen atoms and the oxygen atom combine to form (mainly) the molecular orbitals of the water molecule. Similar information is given in Table 2.6.

The table specifies the components of the atomic orbitals of hydrogen and oxygen (column 1), the applied symbols[6] (column 3) and selected features (columns 2,4,5). The energy relationships between these orbitals of the water molecule, which can be determined by various quantum-mechanical methods,[7] are illustrated in approximate form in Figure 2.5 (detailed values of the potential energy of electrons in the various molecular orbitals of water are analyzed further and presented in Table 2.7).

In accordance with the information and conventions given in Figure 2.4 and in Table 2.6, we can present the electron configuration of the H_2O molecule in the ground state (in the same way as above for the hydrogen and

[6] For clarity's sake, we should add that the system of symbols used here to describe molecular orbitals is one of many. In the spectroscopic literature we can find many other ways of denoting energy states and molecular orbitals, depending on the quantum-mechanical calculation method or the type of spectroscopic analysis.

[7] One such simple method, described in relation to the H_2O molecule, by Haken and Wolf (1995) among others, involves the application of group theory, which describes the action of so-called symmetry operators on the wave functions of electrons. Another very efficient method is the one using RHF (the restricted Hartree–Fock wave function) (see, e.g., Chaplin (2006)).

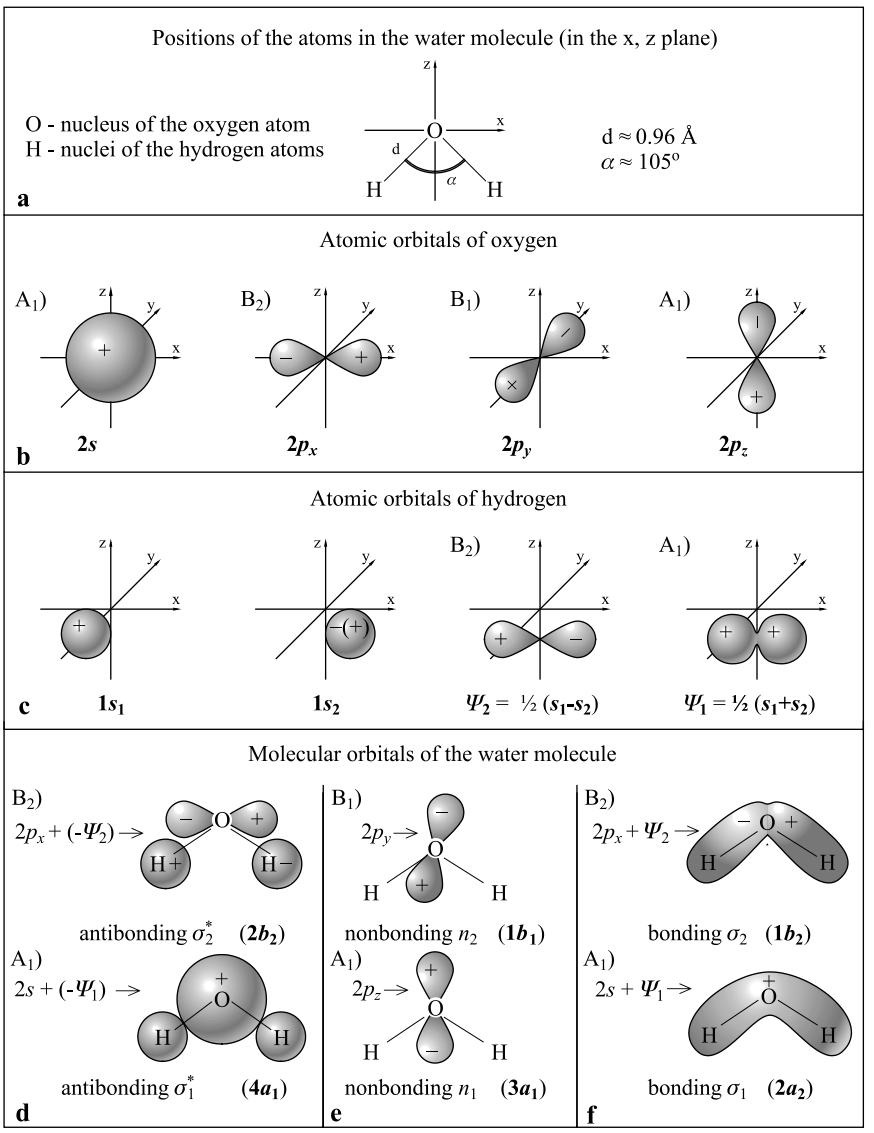

FIGURE 2.4. Sketches of the atomic orbitals of hydrogen and oxygen, and the molecular orbitals of the water molecule (explanation in the text).

oxygen atoms) in the form of the following sequence of orbitals of increasing energy,

$$-\,\text{water:}\underbrace{[1a_1^2],\quad [2a_1^2, 1b_2^2, 3a_1^2, 1b_1^2]}_{HOMO},\quad \underbrace{4a_1 2b_2 \ldots}_{LUMO}.$$

TABLE 2.6. List of symbols and features of the molecular orbitals of H_2O (MO) and the input orbitals of hydrogen and oxygen forming them (input AO).

		MO			
Input AO	Symmetry types	Symbols	Functions[a]	Occupations in ground state[b]	
-1-	*-2-*	*-3-*	*-4-*	*-5-*	
1*s* Hydrogen and $2p_x$ Oxygen	B_2	$2b_2$	σ_2^*	LUMO	
1*s* Hydrogen and 2*s* Oxygen	A_1	$4a_1$	σ_1^*		
$2p_z$	B_1	$1b_1$	n_2	HOMO	Valence orbitals
$2p_y$	A_1	$3a_1$	n_1		
1*s* Hydrogen and $2p_x$ Oxygen	B_2	$1b_2$	σ_2		
1*s* Hydrogen and 2*s* Oxygen	A_1	$2a_1$	σ_1		
1*s* Oxygen	A_1	$1a_1$	n_0		

[a] Division according to the bonding ability of the atoms in the molecule (as used later in this book to describe the functions of electrons in large organic molecules): bonding (σ), nonbonding (n), and antibonding (σ*);
[b] Division in terms of the occupation of the various electronic orbitals: highest occupied molecular orbitals (HOMO) or lowest unoccupied molecular orbitals (LUMO).

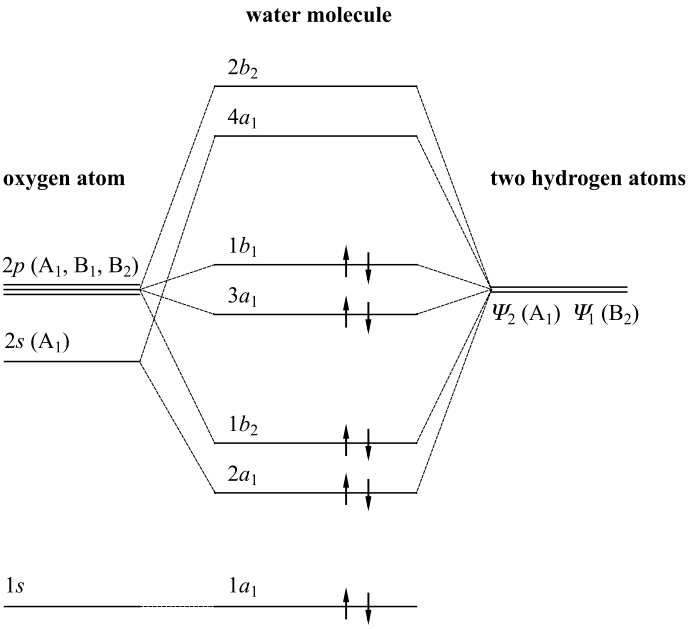

FIGURE 2.5. The energy levels of a water molecule and its constituent atoms: one atom of oxygen and two atoms of hydrogen. The pairs of vertical arrows on the energy diagram of the water molecule illustrate the distribution of electron pairs (with opposite spins) in this molecule in its ground state. Ψ_1 and Ψ_2 denote the electron wave function of the two hydrogen atoms: $\Psi_1 = 1/2(s_1 + s_2)$ and $\Psi_2 = 1/2(s_1 - s_2)$. The symbols in parentheses next to the energy levels denote the relevant types of symmetry (see text).

TABLE 2.7. Energies of the electrons in a water molecule [eV] described by different molecular orbitals and defined by various authors.*

							Water	Ions		
							Dimer	H_3O^+–H_2O	H_3^+–H_2O	
		Orbital	Gas	Liquid	Ice	Orbital	H_2O–H_2O	C_s Symmetry	C_2 Symmetry	HO^-–H_2O
	-1-	*-2-*	*-3-*	*-4-*	*-5-*	*-6-*	*-7-*	*-8-*	*-9-*	*-10-*
A	LUMO	$3b_2$	+28.0[1]							
		$2b_2$	+8.0[1]							
						$4a_1$ proton donor	+7.3[1]	+0.6[1]	+0.5[1]	
		$4a_1$	+6.0[1]			$4a_1$ proton acceptor	+5.3[1]	−0.9[1]	−0.7[1]	+12.6[1]
B	HOMO	$1b_1$	−12.6[2]	−11.16[8]	−12.3[4,5]					
			−14.0[1]		−11.8[6]	$1b_1$ proton donor	−12.7[1]	−21.0[1]	−21.9[1]	−3.2[1]
						$1b_1$ proton acceptor				
						$3a_1$ proton donor	−14.1[1]	−22.6[1]	−21.9	−3.2[1]
		$3a_1$	−14.84[8]	−13.50[8]	−14.2[4,5]	$3a_1$ proton donor				
			−14.80[2]			$1b_1$ proton acceptor	−14.8[1]	−23.4[1]	−23.1[1]	−6.0[1]
			−15.0[1]			Major $3a_1$ proton acceptor				
						Minor $1b_2$ proton donor	−16.3[1]	−26.9[1]	−27.8[1]	−7.0[1]
		$1b_2$	−18.78[8]	−17.34[8]	−17.6[4,5]	Major $1b_2$ proton donor	−18.7[1]	−28.7[1]	−27.8[1]	−7.0[1]
			−18.60[2,8]		−18.0[7]	Minor $3a_1$ proton acceptor				
			−19.0[1]			$1b_1$ proton acceptor	−20.2[1]	−29.0[1]	−28.8[1]	−11.3[1]
		$2a_1$	−32.62[8]	−30.90[8]	−31.0[6]	$2a_1$ proton donor	−35.8[1]	−44.0[1]	−44.6[1]	−25.1[1]
			−32.60[2]			$2a_1$ proton acceptor	−37.4[1]	−46.3[1]	−45.5[1]	−28.7[1]
			−37.0[1]							
		$1a_1$	−559[1]	(−559[1])	(−559[1])	0-atom 1*s* proton donor	−558.4[1]	−566.7[1]	−567.6[1]	−549.0[1]
						0-atom 1*s* proton acceptor	−560.1[1]	−568.6[1]	−567.6[1]	−551.6[1]
C	Rydberg states	$3pb_1$	−2.43[3]							
		$4sa_1$	−2.00[3]							
		$3pa_1$	−2.62[3]							
		$3sa_1$	−5.18[3]							

* References: (1) Chaplin 2006; (2) Banna et al. 1986; (3) based on data in Mota et al. 2005; (4) Henderson 2002; (5) Krischok et al. 2001; (6) Shibaguchi et al. 1977; (7) Campbell et al. 1979; (8) Winter et al. 2004.

The first component of each designation stands for the consecutive number of the orbital belonging to a given type of molecular symmetry[8] (A_1 or B_1 or $B_{2;}$ see column 2 in Table 2.6). The letter in position two of the designation (a_1 or b_1 or b_2) with the subscript repeats the symbol for the type of symmetry. The remaining denotations are as for atomic orbitals (see above).

As we can see, we can distinguish two groups of orbitals: HOMO, the highest-energy occupied molecular orbitals, which in the ground state of the water molecule are occupied by electrons, and LUMO, the lowest unoccupied molecular orbitals, which in the ground state are unoccupied. They come about as the combination of different O and H atomic orbitals (see Figures 2.4 and 2.5), they have various properties, and fulfill various functions (see Column 4 in Table 2.6). The first of these HOMOs, $1a_1$, a nonbonding orbital (n_0), arises from the inner atomic orbital of oxygen ($1s$) and in fact duplicates it (i.e., the symmetry of the electronic charge distributions is practically spherical with respect to the oxygen nucleus). The next HOMO, $2a_1$, is a contribution from the $2s$ orbital of the oxygen atom (and only partially a contribution from the 1s atomic orbitals of hydrogen, or to be exact, their functions Ψ_1; see Figure 2.4c), respectively, and so is approximately spherical. The next three HOMOs—$1b_2$, $3a_1$, and $1b_1$—are orthogonal around the oxygen atom and without obvious sp^3 hybridization[9] characteristics. But the highest-energy HOMO, $1b_1$, is predominantly p_z in character, with no contribution from the hydrogen 1s orbital, and contributes mainly to the so-called "lone pair" effects. It thus has the character of a nonbonding orbital (n_2). Orbitals $2a_1$, $1b_1$, and $3a_1$ all contribute to the O–H bonds; $3a_1$, however, formed as it is mainly from the p_y orbital of oxygen, is only weakly bonding, so we can assume it to be nonbonding (n_1). In contrast, the O–H bond is based mainly on two σ-type bonding orbitals, that is, on orbital $1b_2$, which is strongly bonding (σ_2), and on orbital $2a_1$, which is formally bonding (σ_1), but weakly so.

In addition to these five HOMOs, the next, energetically higher orbitals $4a_1$ and $2b_2$, mentioned in Table 2.6, and also the orbitals of even higher energies, such as $3b_2$, not accounted for in this table, are unoccupied in the ground state, and are therefore classified as LUMOs. They are antibonding orbitals (σ^*-type). $4a_1$ and $2b_2$ are O–H antibonding orbitals. They have the greatest electron densities around the O atom, whereas orbital $3b_2$ has the greatest electron density around the H atom.

---

[8] Representations of A_1, B_1, B_2, and others linked with this type of molecular symmetry are described in the monographs by Barrow (1969) and Haken and Wolf (1995), among others.

[9] By hybridization we mean the situation when a molecular orbital arises when different types of atomic orbital mix, in this particular case the $2p$ orbital of oxygen and the $1s$ orbital of hydrogen.

We should add that we can predict these HOMOs and LUMOs for water fairly easily from the description of electronic wave functions if we avail ourselves of symmetry operators and group theory (see, e.g., Haken and Wolf (1995)). The set of these orbitals is a kind of fundamental base set. But the diversity and complex electronic nature of the water molecule are such that there are yet further series of interactive electronic states (molecular orbitals) resembling the main ones. We address this particular question a little later.

Energy States of Electrons

Tables 2.7A and B, columns 3, 4, and 5, list the electronic energy values characteristic of all three states of aggregation and described by HOMO and LUMO orbitals. These values were determined by various authors, usually with a method employing RHF (restricted Hartree–Fock wave function; see, e.g., Chaplin (2006)). Obviously, the energies of all bonding and nonbonding electrons in HOMO are negative; those in LUMO are positive.

It is worth noting that in a natural environment, apart from single molecules of water, not interacting among themselves, various kinds of supramolecular structures can occur (Eisenberg and Kauzmann 1969, Dera 2003, Chaplin 2006). These larger structures can be electrically neutral (dimers, polymers, crystalline elements), but also electrically charged (ions and their combinations). This applies in larger or smaller measure to water in all its three states: gaseous water (water vapor), liquid water, and ice. It is also the reason for the formation of a complex series of electronic states, quantitatively very different from the states of the single molecule mentioned earlier. Some of these states and their characteristic energy values are also given in Table 2.7, columns 6 to 10.

It is clear from these data that the energy differences between these main HOMO and LUMO electronic energy states of the water molecule and its supramolecular structures are very great: of the order of tens or hundreds of eV. The least of these differences is almost 20 eV. This implies that the absorption or emission of radiation of very short wavelengths, usually shorter or very much shorter than 100 nm, is responsible for electronic transitions between these states. However, as we show in due course, water absorbs, as a result of electronic transitions, not only very short waves (i.e., high-energy photons) but also waves from the $\lambda > 100$ nm range. The absorption of these longer waves may be the result of transitions between the principal energy states, such as are listed in Tables 2.7A and B. We explain below the question of absorption due to electronic transitions of photons from the $\lambda > 100$ nm range.

Interactive Orbitals and Rydberg States

As we stated above, in addition to the main HOMO and LUMO electronic energy states listed in Tables 2.7A and B, the diversity and complex

electronic nature of the water molecule means that it is further characterized by a whole series of interactive electronic states (molecular orbitals) similar to the main ones, for example, $3a_1$-like orbitals, $4a_1$-like orbitals, and so on. Among these, the so-called Rydberg states (and their corresponding orbitals) of electrons play a particularly important part in the formation of electronic absorption spectra of water (see, e.g., Haken and Wolf (1996, 2002) and Mota et al. (2005)). They occur in both atoms and molecules, and usually refer to a few (one or two) of the outermost valence electrons. We recall that this is connected with the change in the electronic configuration of an atom (both isolated and as a component of a molecule).

These are highly excited electronic states, described by orbitals whose dimensions are large in comparison with those of the core of the atom or molecule in the ground state. This means that when one of these outermost electrons is excited to a very high energy level, it enters a spatially extensive orbit, that is, an orbital that is situated much farther away from the core than the orbitals of all the other electrons. This excited electron then acts from this great distance upon the atomic or molecular core, consisting of the nucleus (or nuclei) and all the other electrons, as if it were practically a point charge, equal to 1 (+1e), that is, the same charge as that of the hydrogen nucleus. As long as the excited electron does not approach the atomic or molecular core too closely, it behaves as though it belonged to a hydrogen atom. Hence, the behavior of "Rydberg" atoms and molecules is in many respects similar to that of highly excited hydrogen atoms. In particular, the relationship between the electronic energy E_n and the number n (the principal quantum number) of the Rydberg orbit resembles, after correcting for the so-called quantum defect, that for the hydrogen atom and takes the form:

$$E_n = hcR_y \frac{z_e}{(n-\delta)^2} - E_i, \tag{2.5}$$

where z_e is the core charge ($z_e = 1$), E_i is the ionization energy of a given electron, R_y is 109677.5810 cm^{-1} the Rydberg constant, δ is the quantum defect resulting from the penetration of the Rydberg orbital into the core.

The codes used to describe Rydberg orbitals are also similar to those used for atomic orbitals. First we write the principal quantum number n (i.e., the number of the Rydberg orbit), then the denotation of the subshell (s, p, d, . . .), and finally the type of electron. So for water we have the following.

$n\ s\ a_1$ (n = 1,2, . . .), $n\ p\ a_1$ (n = 1,2, . . .) with respect to the orbital of a valence electron of symmetry A_1;

$n\ s\ b_1$ (n = 1,2, . . .), $n\ p\ b_1$ (n = 1,2, . . .) with respect to the orbital of a valence electron of symmetry B_1.

Studies have shown that in the case of the water molecule, the following four Rydberg states most probably exist (see, e.g., Mota et al. (2005)): $3sa_1$, $3pa_1$, $4sa_1$ and $3pb_1$.

The values of the quantum defect δ appearing in Equation (2.5) depend on two quantum numbers: n (the number of the orbit) and 1 (the orbital quantum number, equivalent to the type of subshell: s, p, d, etc.) and are usually determined empirically. Mota et al. (2005) obtained these values for the above-mentioned frequent states of the water molecule: $\delta(3sa_1) = 1.31$, $\delta(3pa_1) = 0.72$, $\delta(4sa_1) = 1.39$, and $\delta(3pb_1) = 0.65$. The electronic energies characteristic of these Rydberg states of the water molecule, calculated on this basis using Equation (2.5), are given in Table 2.7C. In these calculations it was assumed that the ionization energy with respect to the individual electrons is respectively equal to (see Table 2.1, items 19 and 20) minus the bonding energy of electron $3a_1$, which is c. 14.73 eV for states from the series nsa_1 and npa_1, and minus the bonding energy of electron $1b_1$, which is c. 12.62 eV for states from the series npb_1.

As we can see from the energies of electrons in Rydberg states (Table 2.7C) and in HOMO states $3a_1$ and $1b_1$ (Table 2.7B), the energy differences between these two types of orbitals are relatively small and may explain the formation of absorption (emission) spectra in the $\lambda > 100$ nm range. Transitions between these two types of states do not, however, explain the absorption of higher-energy light quanta ($\lambda < 100$ nm): these are absorbed as a result of the photodissociation, photoionization, and photolysis of water (see below).

Electronic Absorption Spectra of the Water Molecule

The direct empirical study of the electronic absorption spectra of water is an extremely complicated matter, and is, moreover, encumbered with considerable error. This is because these spectra are located in the far ultraviolet, a region difficult to access with classical spectroscopic techniques. The results of measurements in the form of photoabsorption spectra obtained for water vapor by means of synchrotron radiation (Mota et al. 2005), or determined indirectly from spectral data for liquid water on the real and imaginary parts of the dielectric function measured by X-ray scattering (Hayashi et al. 2000) are illustrated in Figures 2.6a–d. The figures show that the electronic photoabsorption spectrum consists of:

- One principal, very wide, practically continuous band[10] with a maximum at c. 65 nm (other authors give a slightly different position for this maximum), which, as research has confirmed, is characteristic of water in all three states of matter.
- A number of distinct discrete features (see the positions of bands A, B, and C in Figure 2.6) located in the spectral region around $\lambda > 100$ nm, which are especially conspicuous for water vapor.

[10] Except for certain discontinuities in the region c. 80 nm, which have not been examined in detail; they may well be involved in the photoionization of the electron $3a_1$.

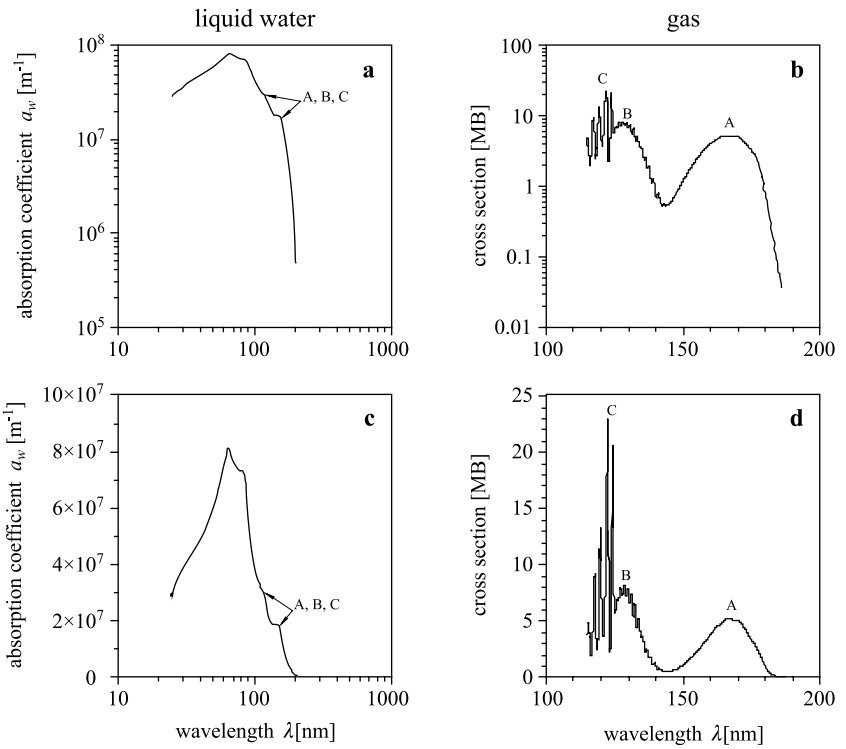

FIGURE 2.6. Electronic UV absorption spectra of water: absorption coefficient spectra of liquid water on a logarithmic scale (a) and a linear scale (c), determined from spectral data of the real and imaginary parts of the dielectric function measured by inelastic X-ray scattering (by Hayashi et al. (2000)); spectral absorption cross-section of water vapor on a logarithmic scale (b) and a linear scale (d), determined using synchrotron radiation (based on Mota et al. (2005)). MB = Mega Barn = 10^{-20} m^2 per 1 molecule.

The reason for the occurrence of this wide, almost continuous, principal photoabsorption band is as follows. It consists mainly of superposed absorption spectra of high-energy photons causing photoionization and photodissociation, which are continuous in the case of energies higher than the ionization and dissociation energies. In the shortwave region of the electromagnetic spectrum (γ and X-radiation), we have continuous absorption of photons photolyzing water.

There is no doubt that further discrete subbands, corresponding to electronic transitions between (suitably distant) discrete energy levels, are also components of this band. Figures 2.6a and c show, however, that these discrete features are not particularly conspicuous (apart from the distinct discontinuity around 80 nm mentioned in footnote 10) in this wide continuous band, which is similar for water in all its states of matter. The huge diversity

and spectral differentiation of these discrete features, as well as their vast numbers, are further reasons for their inconspicuousness.

Overlapping this wide continuous band are several, more subtle features that are characteristic of the water molecule, mostly in the gas state (see Figures 2.6 b and d).

A: A relatively wide subband in the 145–180 nm region with a maximum at c. 166.5 nm
B: A relatively wide subband in the 125–145 nm region with a maximum at c. 128 nm
C: A set of narrow bands in the 115 nm–c. 125 nm region

All these three features of the light absorption spectra were obtained empirically by means of synchrotron radiation and analyzed in detail (see Table 2.8) by Mota et al. (2005). Among other things, they showed that subband A (145–180 nm) is the result of the $1b_1 \rightarrow 4a_1$-like orbital transition, which has been shown to dissociate water into OH + H. This band has an electronic-vibrational structure, even though it is very broad and not particularly conspicuous. The positions of these fine-structural features of subband A in the absorption spectrum, along with the more important results of this vibrational analysis are given in Table 2.8A and illustrated in Figure 2.7. This band is also partially overlapped by a Rydberg structure (among others, absorption corresponding to the $1b_1 \rightarrow 3sa_1$ transition; see below).

Subband B (125–145 nm), also involved in photodissociation, is generated by the excitation of electron $3a_1$ and to a lesser extent by the excitation of electron $1b_1$ to the Rydberg level $3sa_1$; these are therefore the $3a_1 \rightarrow 3sa_1$ and $1b_1 \rightarrow 3sa_1$ transitions, that is, from the Rydberg series. Unlike subband A, this one has a very distinct vibrational structure (see Figure 2.8), the most significant features of which are listed in Table 2.8B.

Finally, the set of narrow bands C (from 115 nm to c. 125 nm) is an extension of the system of Rydberg transitions in bands A and B and corresponds to the following two systems of these transitions:

- Rydberg series converging to the lowest ionic ground state, which correspond to electronic transitions from the $1b_1$ state to Rydberg states of types nsa_1 (mainly for $n = 3$ and $n = 4$), npa_1 (mainly for $n = 3$), and npb_1 (mainly for $n = 3$)
- Rydberg series converging to the second ionic ground state, which come into being as a result of electrons $3a_1$ being excited to Rydberg states $3sa_1$

Both systems in these series have an intricate vibrational structure (Figure 2.9), associated mainly with mode II vibrational transitions, that is, bending, and to a lesser extent with mode I transitions or stretching. The positions of the absorption maxima due to these electronic transitions, together with the various changes in the vibrational states accompanying them, are given in Tables 2.8C and D. Both of these Rydberg series have a natural boundary on

TABLE 2.8. The principal structural elements in the absorption spectrum of a water molecule in the range from c. 110 to c. 180 nm.

A. Some energies and wavelengths of photons absorbed as a result of $1b_1 \rightarrow 4a_1$ type transitions with simultaneous changes in vibrational quantum numbers ($\Delta\upsilon_1$, $\Delta\upsilon_2$, $\Delta\upsilon_3$,) in subband A

No.	Assignment	Energy [eV]	λ [μm]
-1-	*-2-*	*-3-*	*-4-*
1	0,0,0	7.069	0.175
2	0,1,0	7.263	0.171
3	0,2,0 1,0,0	7.464	0.166
4	0,3 0	7.668	0.162
5	0,4,0 2,0,0	7.872	0.158
6	0,5,0	8.067	0.1537
7	0,6,0 3,0,0	8.260	0.150
8	0,7,0	8.463	0.147
9	4,0,0	8.604	0.144
10	0,8,0	8.658	0.143

B. Some energies and wavelengths of photons absorbed as a result of $1a_1 \rightarrow 3sa_1$ type transitions with simultaneous changes in vibrational quantum numbers ($\Delta\upsilon_1$, $\Delta\upsilon_2$, $\Delta\upsilon_3$,) in subband B

No.	Assignment	Energy [eV]	λ [μm]
-1-	*-2-*	*-3-*	*-4-*
1	0,0,0	8.598	0.144
2	0,1,0	8.658	0.143
3	0,2,0	8.775	0.141
4	0,3,0	8.875	0.140
5	0,4,0	8.978	0.138
6	0,5,0	9.083	0.137
7	0,6,0	9.198	0.135
8	0,7,0	9.294	0.133
9	0,8,0	9.393	0.132
10	0,9,0	9.479	0.131
11	0,10,0	9.574	0.130
12	0,11,0	9.671	0.128
13	0,12,0	9.770	0.127
14	0,13,0	9.864	0.126
15	0,14,0	9.995	0.124

C. Some energies and wavelengths of photons absorbed as a result of transitions of electron $1b_1$ to selected Rydberg levels with simultaneous changes in vibrational quantum numbers ($\Delta\upsilon_1$, $\Delta\upsilon_2$, $\Delta\upsilon_3$,) (band set C)

No.	Assignment	Energy [eV]	λ [μm]
-1-	*-2-*	*-3-*	*-4-*
1	$3s\ a_1$	7.464	0.166
2	$4s\ a_1$	10.624	0.117
. . . . .			
1	$3p\ a_1$+(0,0,0)	10.011	0.124
2	$3p\ a_1$+(0,1,0)	10.179	0.122
3	$3p\ a_1$+(0,2,0)	10.354	0.120
4	$3p\ a_1$+(1,0,0)	10.401	0.119
5	$3p\ a_1$+(0,3,0)	10.476	0.118
6	$3p\ a_1$+(1,1,0)	10.556	0.117
7	$3p\ a_1$+(1,2,0)	10.721	0.116
. . . . .			
1	$3p\ b_1$+(0,0,0)	10.163	0.122
2	$3p\ b_1$+(0,1,0)	10.360	0.120
3	$3p\ b_1$+(0,2,0)	10.556	0.117
4	$3p\ b_1$+(1,0,0)	10.574	0.117
5	$3p\ b_1$+(0,3,0)	10.763	0.115
6	$3p\ b_1$+(1,1,0)	10.777	0.115

D. Some energies and wavelengths of photons absorbed as a result of transitions of electron $3a_1$ to selected Rydberg levels with simultaneous changes in vibrational quantum numbers ($\Delta\upsilon_1$, $\Delta\upsilon_2$, $\Delta\upsilon_3$,) (band set C)

No.	Assignment	Energy [eV]	λ [μm]
-1-	*-2-*	*-3-*	*-4-*
1	$3s\ a_1$+(0,0,0)	9.991	0.124
2	$3s\ a_1$+(0,1,0)	10.142	0.122
3	$3s\ a_1$ +(0,2,0)	10.320	0.120
4	$3s\ a_1$+(1,0,0)	10.384	0.119
5	$3s\ a_1$+(0,3,0)	10.458	0.119
6	$3s\ a_1$+(1,1,0)	10.516	0.118
7	$3s\ a_1$+(0,2,0)	10.777	0.115

[a] Selected results of analyses; taken from Mota et al. (2005).

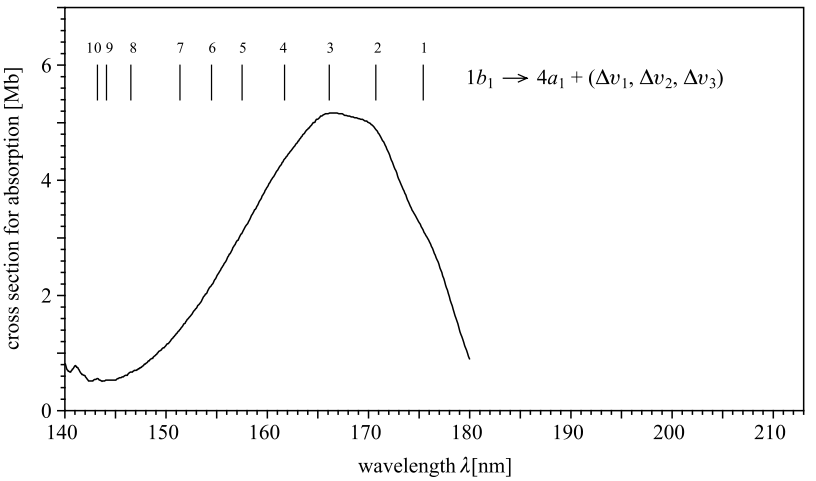

FIGURE 2.7. H_2O molecule photoabsorption spectrum in the A-band (from 145 to 180 nm) with some vibrational series labeled (numbers correspond to Table 2.8A). (Based on data from Mota et al. (2005).)

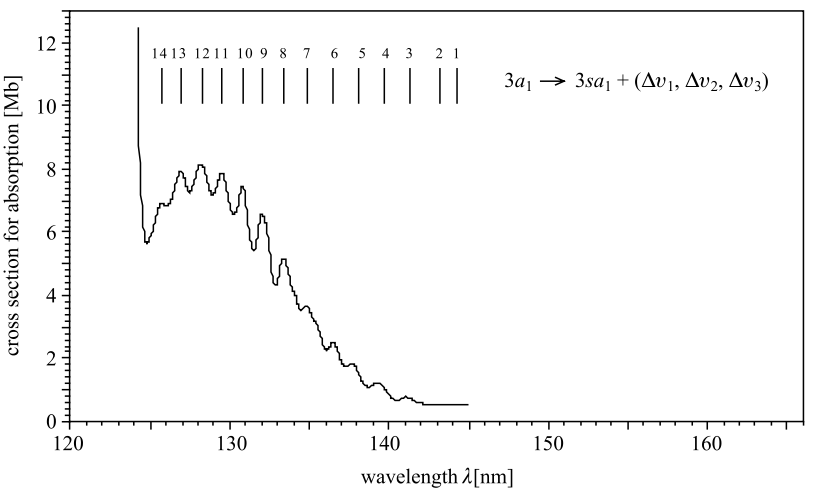

FIGURE 2.8. H_2O molecule photoabsorption spectrum in the B-band (from 125 to 145 nm) with some vibrational series labeled (numbers correspond to Table 2.8B). (Based on data from Mota et al. (2005).)

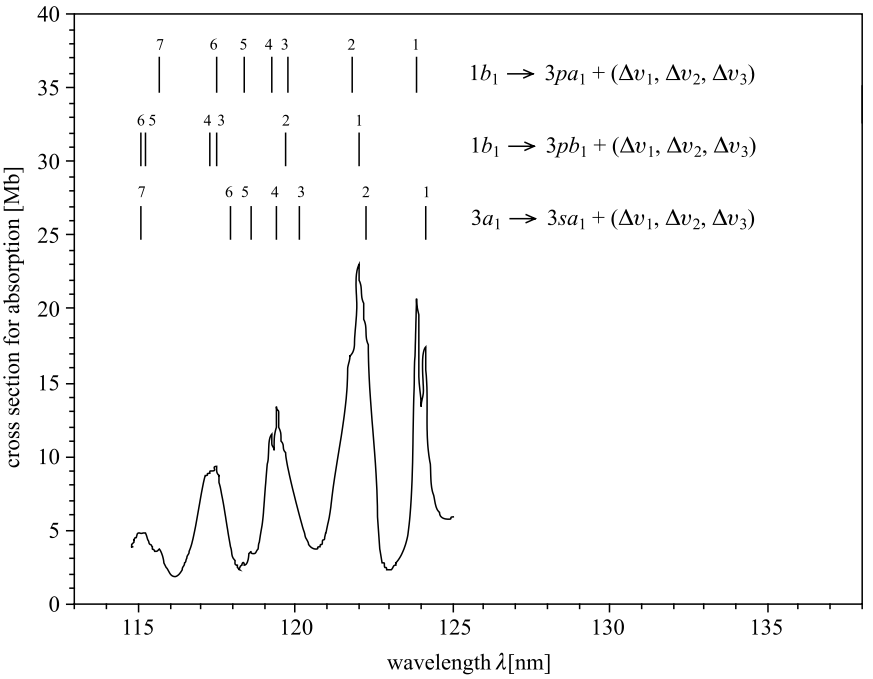

FIGURE 2.9. H_2O molecule photo-absorption spectrum in band set C (from 115 to 125 nm) with Rydberg series labeled and some vibrational excitation modes designated (numbers correspond to Tables 2.8C and D). (Based on data from Mota et al. (2005).)

the shortwave side of the spectrum. The maximum photon energies due to this boundary are equal to the energies of the ionizations that detach individual valence electrons from the molecule:

- Electron $1b_1$, whose ionization energy (minus the bond energy) is c. 12.62 eV (see Table 2.1 item 19; after Lias (2005)), that is, $\lambda \approx 98.3$ nm for the first of these Rydberg series types.
- Electron $3a_1$, with an ionization energy of c. 14.73 eV (see Table 2.1 item 20; after Diereksen et al. (1982)); that is, $\lambda \approx 84.2$ nm for the second of these Rydberg series types.

Clearly, these ionizations can also be caused by the absorption of higher-energy photons (from the shortwave range) and this excess energy would be converted, for example, into the kinetic energy of the released electrons. Such transitions lead to the formation of a continuous spectrum, and that is why a wide band of light absorption by water in this spectral range is observed.

2.2 The Absorption of Light and Other Electromagnetic Radiation in Pure Liquid Water and Ice

Our aim in this section is to characterize the electromagnetic absorption spectra of water in its condensed states, that is, the liquid state (liquid water) and the solid state (ice). A complete explanation of the formation and structure of the absorption spectra of water $a_w(\lambda)$ and of ice $a_{w,ice}(\lambda)$ is not possible on the basis of only what we know from Section 2.1. There we discussed the physical mechanisms of the interaction between electromagnetic radiation and freely moving H_2O molecules not interacting with each other. But these mechanisms provide for a satisfactory explanation of the absorption of such radiation only by water vapor, in which intermolecular interactions are negligible. They are not sufficient for an adequate description of the absorption properties of liquid water and ice, which are substantially modified by these interactions. Moreover, the mechanisms described in Section 2.1 do not explain the absorption of shortwave radiation in the $\lambda < 20$ nm range, that is, very-high-energy UV photons, and X- and γ-radiation quanta. Neither do they explain the absorption of longwave electromagnetic radiation such as radio waves. Section 2.2.1, therefore, extends the material of Section 2.1 by describing the physical principles underpinning the formation of spectra of the absorption of radiation by water in its condensed states.

Sections 2.2.2 and 2.2.3 contain detailed descriptions of the radiation absorption spectra of liquid water and ice. In order to produce them, we analyzed more than 30 empirical spectra of the absorption of radiation by liquid water (both distilled and very clear natural water in seas and lakes)[11] $a_w(\lambda)$ and ice[12] $a_{w,ice}(\lambda)$ in different spectral ranges. On the basis of this analysis and also reviewing the information on the interaction of electromagnetic radiation with water, available in numerous publications, we compiled a list of the spectral features of the absorption of this radiation in water in all its three states (water vapor, liquid water, and ice). Covering a very wide range of

[11] Spectra of $a_w(\lambda)$ or the relevant data enabling them to be determined are available in these publications: Clarke and James (1939), Le Grand (1939), Shuleykin (1959, 1968), Smoluchowski (1908), Ivanov (1975), Zolotarev et al. (1969), Wieliczka et al. (1989), Tam et al. (1979), Sullivan (1963), Sogandares and Fry (1997), Smith and Baker (1981), Shifrin 1988, Segelstein (1981), Quickenden and Irvin (1980), Pope and Fry (1997), Pope (1993), Palmer and Williams (1974), Morel and Prieur (1977), Kopelevitch (1976), Hale and Querry (1973), Buiteveld et al. (1994), Bricaud et al. (1995), Boivin et al. (1986), Baker and Smith (1982), Pelevin and Rostovtseva (2001), Hayashi et al. (2000), and Mota et al. (2005).

[12] Spectra of $a_{w,ice}(\lambda)$ or the relevant data enabling them to be determined are available in these publications: Warren (1984), Perovich and Govoni 1991, Grenfell 1983, 1991, Perovich et al. 1986, Grenfell and Perovich (1981, 1986), Grenfell and Maykut (1977), Irvine and Pollack (1968), and Kou et al. (1993).

radiation wavelengths—from vacuum UV to microwaves—this list is set out in Table 2.9. This gives the positions of the most important absorption bands (columns 3 to 5), together with an assignment of their origin (column 2). The information provided by this table is very useful when discussing the radiation absorption spectra of liquid water and ice, and we make reference to it many times in this section.

2.2.1 Physical Mechanisms of Absorption

We could, in principle, explain the light absorption spectrum of liquid water and ice in terms of the same mechanisms described for water vapor. However, we would have to significantly modify and extend that description in order to take account of the fact that individual liquid water molecules are not independent of each other but interact through intermolecular forces to form groups of molecules held together by hydrogen bonds—these $(H_2O)_n$-type polymers are known as clusters—and other various ionized structures (see, e.g., Horne (1969), Chaplin (2006), and the papers cited therein). Furthermore, in the ice crystal, every H_2O molecule is hydrogen-bonded to its neighbors (see Eisenberg and Kauzmann (1969), Chaplin (2006), and the papers cited therein). As a result, we have a whole range of intermolecular interactions, which strongly and in various ways disturb or modify the configurations of the excited energy states of the molecules. In some aspects, then, the absorption spectra of liquid water and ice do resemble those of free molecules or water vapor, but in many others they diverge quite substantially from the latter. Figure 2.10 illustrates absorption spectra of water over a wide range of wavelengths for all three of its states: liquid water at room temperature $a_w(\lambda)$, a monocrystal of ice at different temperatures $a_{w,ice}(\lambda)$, and the equivalent quantity of atmospheric water vapor[13] $a_{w,v}(\lambda)$.

This figure shows (but see also Figures 2.11 and 2.14) that the absorption spectra of liquid water and ice in the long-wavelength range (VIS and longer) exhibit a series of vibrational-rotational absorption bands as for water vapor, but in distinctly modified form. In contrast to the spectra of water vapor, then, these are *modified* vibrational-rotational absorption bands of water and ice molecules. Apart from the latter, there are also *condensed* phase absorption bands, which are not present in the water vapor spectra. Finally, the absorption of radio waves in liquid water is fairly strong, stronger than in ice or water vapor. We now briefly discuss the origin of these three characteristic features of the absorption spectra of water in its condensed states. To end this section, we also outline the absorption of shortwave radiation in water,

[13] The equivalent absorption coefficients for water vapor $a_{w,v}(\lambda)$, were determined on the basis of known approximate specific absorption coefficients for water vapor $a^*_{w,v}(\lambda)$ (see Figure 2.3) from the relationship $a_{w,v}(\lambda) = a^*_{w,v}(\lambda)\, C_{w,v}$, where $C_{w,v}$ is the equivalent (for liquid water) concentration of water vapor, equal to 1000 kg m^{-3}.

TABLE 2.9. The more important spectral features of the absorption of electromagnetic radiation in water vapor, liquid water, and ice (type Ih).

No.	Assignment	Water vapor[a]	Liquid water[a]	Ice (type Ih)[a]
-1-	*-2-*	*-3-*	*-4-*	*-5-*
1	T_B - intermolecular bend (translation)	—	~200 μm weak wide band	166 μm intense band
2	T_S - intermolecular stretch	—	~50–55 μm very intense band (local maximum)	44 μm very intense band (distinct local maximum)
3	Rotation	~ 118.6, ~70, ~50 μm three very intense bands (absolute maximum in longwave range)	—	—
4	Rotation (for water vapor) L_1 - librations (for liquid water and ice)	27.9 μm intense band (distinct local maximum)	25 μm weak band	~20 μm weak band
5	Rotation (for water vapor) L_2 - librations (for liquid water and ice)	From 16 to 23 μm three weak bands	15 μm very intense wideband (from 11 to 33 μm) (distinct local maximum)	11.9 μm very wide band (distinct local maximum)
6	Vibrational υ_2 - bend (fundamental band Mode II)	6.27 μm several very intense bands in the region from 5 to 7 μm (local maximum)	6.08 μm intense band with a half-width of c. 0.30 μm (local maximum)	6.06 μm weak wide band
7	Vibrational υ_2 - bend + L_2 and associated band		4.65 μm intense band with a half-width of c. 1.3 μm	4.41 μm weak wide band
8	Vibrational 2 υ_2 - bend (overtone) (0,0,0) → (0,2,0)	3.17 μm intense absorption band		
9	Vibrational υ_1 - symmetrical stretch (fundamental band Mode I)	2.73 μm weak band	3.05 μm very intense band	3.24 μm very intense, structurally complex wideband
10	Vibrational υ_3 - asymmetrical stretch (fundamental band Mode III)	2.66 μm very intense band (strong local maximum)	2.87 μm very intense band	3.08 μm (absolute maximum in longwave range)

2.68 μm so-called X-band

A very intense band with a half-width of c. 0.60 μm combined with a maximum in the 2.90–3.00 μm region (absolute maximum in longwave range)

11	Vibrational combination transitions (0,0,0) → (a,1,b); a + b = 1	1.88 μm intense band in the 1.76–1.98 μm region so-called Ω - band	1.94 μm intense band (local maximum)	~2.00 μm weak band (local maximum)
12	Vibrational combination transitions (0,0,0) → (a,0,b); a + b = 2	1.38 μm intense band in the 1.32–1.50 μm region so-called Ψ - band	~1.44 μm intense band (local maximum)	1.50 μm weak band (local maximum)
13	Vibrational combination transitions (0,0,0) → (a,1,b); a + b = 2	1.13 μm intense band in the 1.10–1.17 μm region so-called Φ - band	1.20 μm weak band (bulge)	1.27 μm weak band (local maximum)
14	Vibrational combination transitions (0,0,0) → (a,0,b); a + b = 3	0.935 μm intense band in the 0.92–0.98 μm region so-called. ρστ- band	0.970 μm weak band (local maximum)	1.04 μm very weak band
15	Vibrational combination transitions (0,0,0) → (a,1,b); a + b = 3	0.810 μm intense band in the 0.79–0.84 μm region so-called 0.8μ - band	0.836 μm very weak band	~0.85 μm very weak band
16	Vibrational combination transitions (0,0,0) → (a,0,b); a + b = 4	0.718 μm intense band in the 0.70–0.74 μm region so-called α - band	0.739 μm weak band (small local maximum)	—
17	Vibrational combination transitions (0,0,0) → (a,0,b); a + b = 5	—	0.606 μm very weak band (bulge)	—
18	Vibrational combination transitions (0,0,0) → (a,0,b); a + b = 6	—	0.514 μm very weak band	—
19	Electronic transition: $1b_1 \rightarrow 4a_1$ like orbital	0.1665 μm (distinct local maximum)	~0.150 μm (distinct local maximum)	~0.143 μm (distinct local maximum)
20	Electronic transitions: $3a_1 \rightarrow 3sa_1$ and $1b_1 \rightarrow 3sa_1$	0.128 μm (distinct local maximum)	—	~0.121 μm weak band
21	Electronic transitions: Rydberg series	0.115–0.125 μm (set of narrow bands)	—	—
22	Different electronic transitions, photo-ionization, photodissociation	0.065 μm intense wide band (absolute maximum)	0.056–0.086 μm intense wide band (absolute maximum)	0.073 μm intense wide band (absolute maximum)

[a] Note: in columns 3–5 wavelengths are expressed in μm.

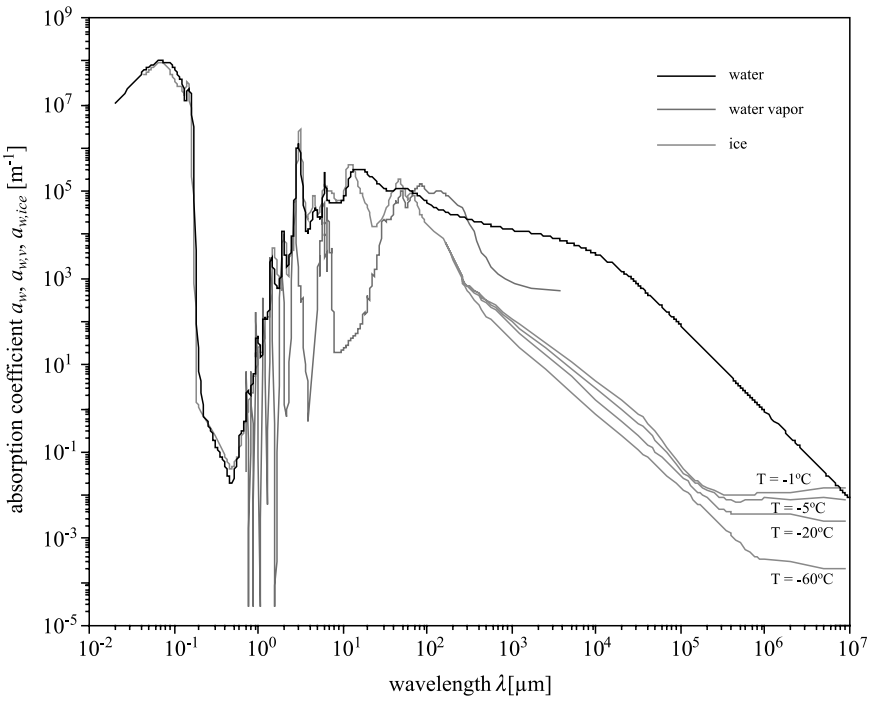

FIGURE 2.10. Absorption spectra in wide range of wavelengths (from UV to short radiowaves): liquid water at room temperature (based on data from Segelstein (1981)); ice crystals at various temperatures (based on data from Warren (1984)); atmospheric water vapor (based on Figure 2.3). (See Colour Plate 1)

that is, the absorption of high-energy UV photons and of X- and γ-radiation, which was not covered in Section 2.1.

Modified Vibrational-Rotational Absorption Bands in Liquid Water and Ice

One would expect that rotations of separate H_2O molecules in the condensed states are to a large extent retarded and sometimes brought to a standstill by the forces acting on the molecules in supramolecular structures and, in theory at least, the resulting vibrational-rotational absorption band structure ought to be less intricate. But this is not so; quite the opposite: in fact, the band structure of condensed phases is very much more complex than that of free molecules. This is because intermolecular interactions give rise to a whole series of vibrational states of the molecules for the same vibrational quantum numbers. These states correspond to a large number of energy levels so close to each other that they form almost a continuum. Hence,

the absorption spectra of these condensed phases, unlike the fine structure of absorption spectra of free H_2O molecules, are practically continuum spectra. As a result these intermolecular interactions, the absorption bands in liquid water and ice, corresponding to diverse vibrational-rotational transitions of the H_2O molecule, are much broadened in contrast to those in water vapor. Moreover, the positions of the wave spectra peaks are shifted in comparison with those of the analogous bands for free single molecules; see the examples in Table 2.10. These shifts are usually in the longwave direction, and in ice are greater than in liquid water. The exception is the fundamental mode II band (bending), which in liquid water and ice is shifted toward the short waves relative to water vapor. The relations between the intensities of the individual bands also vary. For example, according to Eisenberg and Kauzmann (1969), in the gas state, the vibrations involve combinations of symmetric stretch (υ_1, mode I), asymmetric stretch (υ_3, mode III), and bending (υ_2, mode II), of the covalent bonds with absorption intensity $a(\upsilon_1):a(\upsilon_2): a(\upsilon_3) = 0.07:1.47:1.00$. This means that the fundamental mode II band of water in the gas state is the most intense and the fundamental mode I band is the least intense.

However, in the condensed states of water, this situation is radically different. In liquid water the most intense absorption is due to the fundamental mode III band (asymmetric stretch), and the least intense is the mode II band (bending). In liquid water the ratio of these intensities is $a(\upsilon_1):a(\upsilon_2):a(\upsilon_3) = 0.87:0.33:1.00$. For ice these relations are similar to those for liquid water. None of these intricacies characterizing the different positions and intensities of the vibrational-rotational absorption bands in the condensed states as opposed to water vapor are strictly constant; they depend to varying degrees on temperature and pressure, among other things. Detailed treatments of these questions can be found in Eisenberg and Kauzmann (1969), Walrafen (2004), Raichlin et al. (2004), Yakovenko et al. (2002), Worley and Klotz (1966), Symons (2001), Segtnan et al. (2001), Brubach et al. (2005), and elsewhere.

Absorption Bands of Condensed Phases

As we have already mentioned, there appear in the condensed states of water completely new phenomena and interactions between supramolecular structures and electromagnetic radiation that we did not discuss in Section 2.1. Consequently, the absorption spectra of liquid water and ice exhibit a number of features not present in the absorption spectra of water vapor, which may be partially, indirectly, or not at all due to electronic, vibrational, or rotational transitions. The most significant of these features are:

- *Librations* of hydrogen bonds (restricted rotations, or rocking motions). They form two absorption bands: a minor L_1 band with a peak in liquid water at $\lambda \approx 25$ μm and a major L_2 band with a maximum in liquid water at $\lambda \approx 15$ μm. Furthermore, L_1-type librations in combination with the

TABLE 2.10. Positions of the fundamental vibrational-rotational bands of light absorption by water in its various states.

Quantum numbers of excited states	Wavelength λ [nm]		
υ_1, υ_2, υ_3	Water vapor	Liquid water	Ice
-1-	*-2-*	*-3-*	*-4-*
0,1,0	6.27	6.08	6. 06
1,0,0	2.73	3.05	3.24
0,0,1	2.66	2.87	3.08

Based on data from Chaplin (2006), Eisenberg and Kauzmann (1969), and Venyaminov and Prendergast (1997).

principal vibrational transition, that is, (0,0,0) → (0,1,0), produce an absorption band peaking in liquid water at around 4.65 μm. The intensities of these three bands increase with rising temperature, that is, in liquid water together with the falling number of molecules held in clusters by hydrogen bonds. These bands are also characteristic of ice, but are shifted towards shorter waves (see Table 2.10 and also Table 2.9 items 4, 5, and 7). These librations are discussed in greater detail in, for example, Zelsmann (1995), and Eisenberg and Kauzmann (1969).

- *Cluster vibrations*, or translational vibrations: these involve the stretching (T_S) or bending (T_B) of intermolecular hydrogen bonds (O–H . . . O). Intermolecular stretching is responsible for the absorption band centered around 55 μm in liquid water and around 44 μm in ice (see Table 2.9, item 2). Intermolecular bending, however, gives rise to an absorption band at c. 200 μm in liquid water and at c. 166 μm in ice (see Table 2.9 item 1). The higher the temperature is, the less intense the intermolecular stretching bands, but the more intense are the intermolecular bending bands. Cluster vibrations are accorded detailed treatment in Gaiduk and Vij (2001), Brubach et al. (2005), Vij (2003), and Dunn et al. (2006), among others.
- *Molecular vibrations in the crystal lattice* are associated with many absorption bands around $\lambda > 9.5$ μm. These bands are weak in the absorption spectrum of liquid water, but are very distinct, and practically characteristic only of ice. They are due to molecular vibrations in the crystal lattice transmitted by hydrogen bonds as a result of translational ($\lambda > 20$ μm) and rotational (9.5 μm $< \lambda <$ 20 μm) vibrations of the molecules. The reader can find this topic covered in greater detail in Hobbs (1974) and Warren (1984).

Apart from these three features, contributing to the complexity of the absorption properties of liquid water and ice, there are others that affect these properties to a lesser extent. The interested reader is referred to the relevant literature, for example, Johnson (2000), Tsai and Wu (2005), Padró and Marti (2003), Olander and Rice (1972), and Woods and Wiedemann (2004).

Absorption of Radio Waves

This process is typical of liquid water: water vapor and ice absorb radio waves only weakly. We know that electromagnetic radiation of wavelength around $\lambda > 2$ cm (i.e., long microwaves and radiowaves) interacts strongly with the dipoles of H_2O molecules, and that the energy of these interactions is dissipated in the work done shifting these dipoles in the electric field of the wave (see, e.g., Dera (1992)). Quantitatively, then, these interactions depend on the medium in which the radio waves propagate, and in particular on the medium's permittivity, magnetic permeability, and specific electrical conductivity. This problem with regard to aquatic media is discussed in greater depth by Jackson (1975). This author shows that in dipole–electric field interactions energy is absorbed from those frequency ranges in which the period of vibrations is close to the relaxation time of the H_2O dipole: dipole–electric field interactions are therefore relaxation processes. The relaxation time of these dipoles is governed by the forces of intermolecular interactions, which depend strictly on the temperature and pressure of the medium. Although strongly attenuated as a result of friction with adjacent molecules in the medium, these vibrations are maintained by the absorption of radiowaves: the higher their frequency, the stronger is the absorption. This is why radio communication, especially in the shorter wavebands, is difficult in fresh waters and well-nigh impossible in the salt waters of the sea. The radiowave absorption spectra of fresh and salt waters are illustrated in Figure 2.13, curves 2 and 3 (see below).

Absorption of Shortwave Radiation (High-Energy UV, X, γ)

In this book we do not analyze in any great detail the differences between the absorption properties of the three states of water with respect to UV light and radiation of even smaller wavelengths (see Section 2.1.2). Nevertheless, we should mention that these properties are not as well differentiated as those of water regarding visible and longwave radiation. This applies in particular to the very short wave range, where $\lambda < 10$ nm (i.e., mainly X and γ radiation). The absorption properties of these very short waves are determined more by the physical properties of atoms than of molecules. In the spectral interval from around $\lambda < 10$ nm right across to the shortwave range, corresponding to the high-energy quanta giving rise to the photoelectric effect (i.e., $\lambda \approx 23.5$ Å), the absorption properties of water have not, to our knowledge, been investigated empirically.

In contrast, in the wavelength range $\lambda < 23.5$ Å, the absorption spectrum of water in any of its states is very well known, having been studied empirically by the methods of nuclear physics. In this region of the spectrum, high-energy photons of X and γ radiation interact with individual atoms (and their nuclei), successively (with increasing photon energy) giving rise to the photoelectric effect, Compton effect, electron–positron pair formation, and other high-energy processes up to and including intranuclear processes, which were

investigated by nuclear physicists some 40 years ago (see, e.g., the monographs by Aglintsev (1961/1957), Jaeger (1962/1959), Ciborowski (1962), Adamczewski (1965), and others). The absorption coefficient, the wavelength relationship for water in this high-energy spectral range, in which the coefficient is independent of the state of matter of water, is depicted graphically in Figure 2.13, curve 1 (see below). In this spectral region the absorption of radiation falls as the wavelength of the radiation shortens. Detailed information on these interactions of high-energy photons with matter can be found in the classical monographs on nuclear physics and radiation chemistry (see e.g. Wishart and Nocera 1998).

A slightly greater differentiation in the radiation absorption spectra of water in its various states is, however, undoubtedly characteristic as regards UV absorption in the c. 115–180 nm range (see Section 2.1), where the absorption bands are due to Rydberg energy states of the water molecule. The intensity of these absorption bands is distinctly greater for water vapor than for water in its condensed states.

2.2.2 The Absorption of Electromagnetic Radiation in Pure Liquid Water

What we mean here by pure water is a chemically pure substance that consists of water molecules occurring under the natural conditions of Planet Earth: these molecules contain different isotopes of hydrogen and oxygen in their structure. In Nature, the usual structure of the water molecule is $H_2{}^{16}O$; the most common of its isotopic variants are $H_2{}^{18}O$, $H_2{}^{17}O$, and the $HD^{16}O$ heavy water molecule. Occurring in a ratio of roughly 2:0.4:0.3, these last three molecules have a joint concentration in pure water of no more than 0.3% (±0.1%). Natural water also contains even heavier variants of heavy water ($HD^{17}O$, $HD^{18}O$, $D_2{}^{16}O$, $HT^{16}O$, $T_2{}^{16}O$), but only in trace amounts. The proportions in sea waters of the different isotopes of hydrogen and oxygen, and of the several isotopic variants of water are given in Table 2.1 (items 31–39) in accordance with the VSMOW (Vienna Standard Mean Ocean Water) convention.

The electromagnetic radiation absorption spectra of these isotopic variants of pure water differ among themselves, and all differ from the spectra of $H_2{}^{16}O$ water molecules, as numerous authors have shown (Barret and Mansell 1960, Eisenberg and Kauzmann 1969, Janca et al. 2003, Greenwood and Earnshaw 1997, Chaplin 2006). These differences are due to the fact that the molecules of these isotopic variants, with their different masses, all have slightly different geometrical structures and characteristic dimensions. As a result, their dynamic, electric, and magnetic properties (e.g., moments of inertia or dipole moments) also differ, hence the diversity in their energy states. The individual transitions between the energy states of these isotopic variants of water therefore correspond to the absorption of photons of different energies (i.e., different wavelengths).

This is exemplified by the positions of the radiation absorption bands set out in Table 2.4. We see there that the wavelengths of the photons absorbed as a result of these transitions differ for the different isotopic variants of molecules: in the case of water molecules, the wavelengths increase as the molecular mass does so. This differentiation also holds good with respect to absorption due to other types of energy transition—electronic, rotational, and other transitions characteristic of condensed phases (librations, transitional vibrations, and dipole–electric field interactions)—and not just to the positions of the bands and lines in the absorption spectrum, but also to their intensities. Nevertheless, this diversity in the absorption properties of the isotopic variants of water does not significantly affect the total coefficient of radiation absorption $a_w(\lambda)$ of the pure liquid water that fills the oceans and other basins of the Earth. This is because the overall concentration in Nature of this admixture of the isotopic variants of water is generally more than a thousandfold smaller than the concentration of $H_2{}^{16}O$ water. That is why, in our further description of the absorption properties of pure water, we concern ourselves only with the properties of water formed from $H_2{}^{16}O$ molecules.

As we have said, it emerges from the physical principles underlying the formation of the absorption spectra of free H_2O molecules (Section 2.1), and of their aggregations in condensed states (Section 2.2.1), that liquid water (and also water vapor and ice) absorbs ultraviolet strongly and shortwave radiation even more strongly, and on the other hand absorbs infrared radiation strongly and the longer electromagnetic wavelengths even more so. The consequence, therefore, of the arrangement of energy levels specific to the water molecule and its constituent atoms of hydrogen and oxygen is that its radiation absorption spectrum generally consists of two very wide regions of strong absorption—one on the shortwave side and the other on the longwave side of the spectrum—with a relatively narrow absorption minimum in the visible region lying in between (see Figures 2.10, 2.12, and 2.13). This "window" in the spectrum, which has a very high transmittance, lies in the VIS region, and the maximum transmittance, that is, the absolute minimum coefficient of absorption of liquid water $a_w(\lambda)$, lies at a wavelength of c. $\lambda \approx 415$ nm. That, in a nutshell, is how we can characterize the relationships of $a_w(\lambda)$, that is, the light absorption spectrum of water.

A more detailed analysis of the structure of this spectrum of $a_w(\lambda)$ with respect to its several spectral intervals will bring its complexity into focus: this is the next step in our story. To begin with, we describe the fundamental IR absorption bands (spectral range 2.3–8 μm), the absorption of near-IR ($\lambda < 2.3$ μm) and visible light, the absorption of longwave radiation ($\lambda > 8$ μm), and the absorption of UV, X-, and γ-radiation. Then we go on to review the empirical light absorption spectra of liquid water on the basis of the material available in the worldwide subject literature. Finally, we briefly discuss the influence that the absorption of radiation by water has had on the biological evolution of life on our planet.

Fundamental Infrared Absorption Bands (2.3 μm < λ < 8 μm)

The IR, microwave, and radiowave absorption spectrum of liquid water $a_w(\lambda)$ is compared with that of water vapor $a_{w,v}(\lambda)$ in Figure 2.11. This shows that the absorption bands due to fundamental vibrational-rotational transitions (modes I, II, and III, i.e., (0,0,0) → (1,0,0); (0,1,0); (0,0,1)) in pure liquid water molecules are, as a result of these molecular interactions, much broadened in comparison with those in water vapor. In liquid water they are also shifted towards the long waves (except mode II transitions) in comparison with the bands for free molecules in water vapor; see the right-hand part of the plot in Figure 2.11a, and also Table 2.9, items 6–10. This line broadening

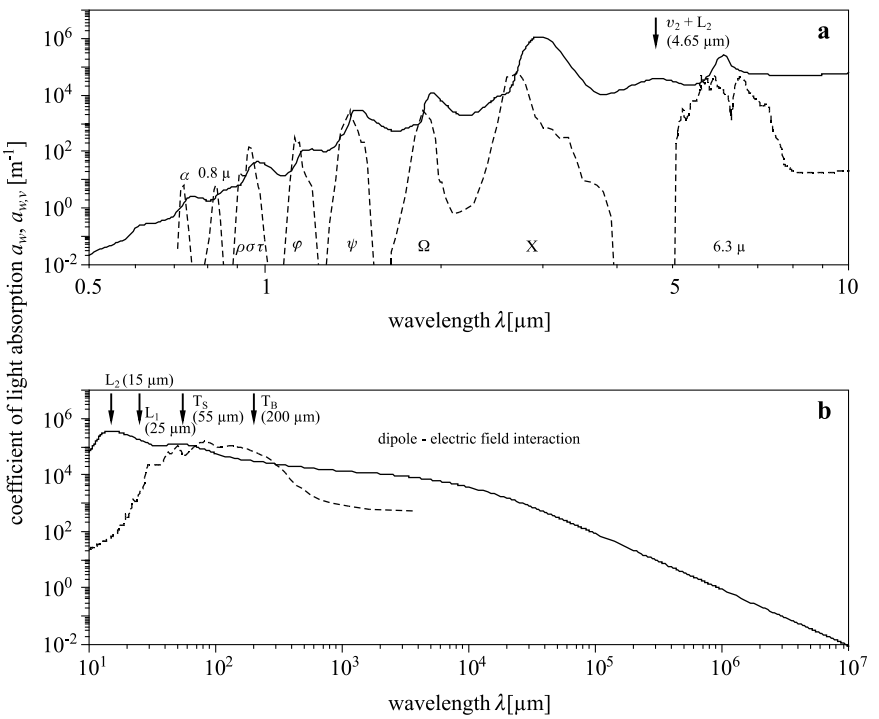

FIGURE 2.11. Visible light-short radio wave absorption spectra of: liquid water – continuous curve (after Segelstein (1981)) and atmospheric water vapor – dashed curve (defined as in the captions to Figs. 2.3 and 2.10);. Explanations: (a) the symbols are the individual water vapor absorption band codes commonly used in atmospheric optics; (a) and (b) the arrows give the positions of the absorption band peaks characteristic of liquid water but not present in the water vapor spectra (T_B, T_S – bands due to transitional vibrations, L_1, L_2 – bands due to librations, $\upsilon_2 + L_1$ - combination bending band (υ_2) in L_2 libration modes; the heading "dipole-electric field interaction" denotes the spectral area of radio wave absorption).

and shift are of such an extent that the absorption bands of liquid water now coalesce to form an absorption continuum.

The strongest absorption band on the longwave side of the spectrum, starting from visible light, lies in the $2.3 < \lambda < 8$ μm wavelength range. Corresponding to the so-called X-band for water vapor, this band is formed in liquid water by combined fundamental mode I and mode III transitions, and peaks at $\lambda = 2.9$–3.0 μm (see Table 2.9, items 9 and 10). It is worth drawing attention to the fact that absorption in this 2.3–8 μm range is more intense, much more intense even, than the corresponding absorption in water vapor. Within this same wavelength range we also observe additional electromagnetic radiation absorption bands that do not occur in the absorption spectrum of free single molecules in water vapor. The most significant of these bands is a wide intense one peaking at $\lambda = 4.65$ μm: it is a combination band of bending (υ_2) and librations (mode L_2; Table 2.9, item 7). The existence of this band is the reason why in the spectral interval between 4 and 5 μm the absorption of radiation by liquid water is on average around 10^4 times greater than the absorption of an equivalent quantity of water vapor comprised of free, noninteracting H_2O molecules.

Absorption of Near Infrared and Visible Light (0.4 μm $< \lambda < 2.3$ μm)

In the wavelength range $\lambda < 2.3$ μm there is a whole series of broad, overlapping absorption bands of pure liquid water, the intensities of which decrease with increasing photon energy (i.e., with shortening wavelength); see Figure 2.11a (left-hand side of the plot) and also Table 2.9, items 11–18; notice that these bands are less intense than the fundamental absorption bands we mentioned earlier. As in the case of discrete H_2O molecules, these bands are due to vibrational-rotational harmonic and combination transitions from the ground state, specified earlier in Figure 2.3a, but they are wider and usually shifted in the direction of the longer wavelengths. Again, as in the case of such molecules, some of these broadened bands lie in the visible range of the spectrum, although there are more of them in the VIS range in the case of liquid water than of water vapor. These include two discernible, although quite weak bands at c. 606 nm and c. 515 nm (See Table 2.9, items 17 and 18). Notice also, that as in the case of the fundamental absorption bands, these harmonic and combination absorption bands of liquid water are generally more intense than those of water vapor. Exceptional here are certain absorption bands of water vapor, principally those designated in the accepted notation of atmospheric optics as α, 0.8μ, ρστ, and φ; see Figure 2.11a. These relatively narrow absorption bands of discrete molecules are characterized by greater intensities than the absorption coefficients of liquid water, although only in narrow ranges around their peaks.

Absorption of Longwave Radiation ($\lambda > 8$ μm)

The longwave absorption spectra ($\lambda > 8$ μm) in liquid water and water vapor in this spectral region differ from each other the most (see Figure 2.11b and the

right-hand side of Figure 2.11a; see also Table 2.9, items 1–5). In this region then, free molecules absorb quite strongly, at a level comparable to that of liquid water only in the c. 50 μm < λ < 300 μm range. The complex absorption bands here are due to vibrational-rotational transitions between various excited states, superimposed on which are bands due to purely rotational transitions.

On the longwave side of this range (at c. λ > 300 μm), light absorption by free molecules in water vapor is more than one order of magnitude smaller than that by liquid water, even though water vapor is also a strong absorber of short radiowaves. On the shortwave side of this range (c. 8 μm < λ < 50 μm) the differences in absorption of water vapor and liquid water are even greater: the absorption coefficients of the latter are three to four orders of magnitude larger than the former. Generally speaking, the absorption coefficients of liquid water are very high right across the IR and microwave regions and do not begin to decrease visibly until we reach the long radiowave region.

Responsible for this absorption are the condensed phase bands (discussed earlier in Section 2.2.1), and not the rotational or vibrational-rotational transitions typical of free H_2O molecules. In liquid water they are librations L_1 and L_2 with peaks at c. 15 μm and c. 25 μm, and the translational vibrations T_S and T_B with peaks at 55 μm and c. 200μm. At even longer wavelengths (microwaves and radiowaves), this absorption in liquid water is caused by dipole–electric field interactions of the H_2O molecules, which we described above (see, e.g., Dera (1992, 2003)). Having such absorption properties, liquid water strongly absorbs electromagnetic radiation across the entire IR, microwave, and radiowave range: pure water is therefore practically opaque to these wavelengths. This extremely important physical property of water plays a fundamental part in its warming by solar radiation and in its evaporation from the surface layer of the oceans, and hence in the overall processes shaping climate and life on the Earth (see, e.g., Trenberth (1992)).

The Absorption of Ultraviolet, X-, and γ-Radiation

As we mentioned in our description of the shortwave region of the electromagnetic spectrum (UV), the absorption of UV light in pure liquid water (and also by water vapor and ice) is due to electronic vibrational-rotational transitions in H_2O molecules, and also to their dissociation and ionization. These processes give rise to certain spectral features of this absorption (see Section 2.1.2, Figures 2.6–2.9, and Table 2.9, items 19–22), namely, a wide absorption band peaking at c. 65 nm and a set of narrower, intricately structured absorption bands lying between c. 115 nm and c. 180 nm. These latter are very strong bands (see, e.g., Figure 2.10), the most intense in the entire electromagnetic spectrum, with absorption coefficients of up to c. 10^8 m^{-1} (at c. 65 nm). These bands are characteristic of water in all its three states, although there is no doubt that the bands in the 115–180 nm range, brought about by Rydberg state changes in the electronic states of the water molecule, are more intense for free molecules (water vapor) than for the condensed phases of water.

Notice that this strong absorption concerns very short wave UV radiation. In contrast, the band intensity for the absorption of longer UV waves ($\lambda >$ 180 nm) plunges by more than nine orders of magnitude (i.e., more than a billion times!), and in the near-UV and the shortwave part of the VIS region oscillates between 10^0 and 10^{-2} m^{-1}. Hence the depth of penetration of VIS radiation in pure sea water (e.g., the Sargasso Sea) is relatively great: c. 100 m. In practical terms, it is only at 100 m and more beneath the surface that the irradiance due visible light drops to 1% of its value at the sea surface. The transmittance of this light is therefore also greater than that of shortwave X and gamma (γ) radiation in the range above $\lambda > 10^{-4}$ Å (see Section 2.2.1). Evidence to support this claim is provided by Figure 2.13, which compares X- and γ-radiation absorption spectra as determined by the methods of nuclear physics (plot 1 in this figure) with the VIS absorption spectrum (see the position of the minimum of plot 2 in this figure).

Empirical Light Absorption Spectra of Liquid Water: A Review

The experimental determination of the light absorption spectra of liquid water is in practice very difficult, both because of the technical problems involved in the direct or indirect measurement of absorption coefficients and the impossibility of obtaining ideally pure water for our research (these questions are discussed more broadly, e.g., by Shifrin (1988) and Dera (2003)). In such investigations it is particularly important to eliminate suspended particles from the water samples to be examined. Light scattering by the tiny quantity of these particles present even in filtered distilled water and in the purest ocean waters (of the order of 1000 particles with diameters in excess of 1 μm (see, e.g., Jonasz and Fournier (1999) and Dera (2003)) can lead to major errors in the measurement of absorption. This is especially significant in studies of VIS and near-UV absorption, where the light absorption coefficients of structurally pure liquid water are very small; they may in fact be smaller than or comparable to the light-scattering coefficients of the suspended particles. Hence, as we show in due course, the absorption of VIS and near-UV light in liquid water measured by various authors are encumbered with serious errors and are frequently very different.

In view of these difficulties, practically the only reliable source of data on light absorption in pure water was for many years the work by Clarke and James (1939). From the light attenuation coefficients that they measured in distilled water $c_w(\lambda)$ in the $375 < \lambda < 800$ nm wavelength range (Table 2.11, column 2) the light absorption coefficients of water $a_w(\lambda)$ in this spectral interval can be determined indirectly with the aid of the relationship (1.2) given in Chapter 1. For this, we also need the relevant light-scattering coefficients in water, $b_w(\lambda)$, determined theoretically by Le Grand (1939). The results of these calculations are given in Table 2.11 (column 3).

In the worldwide subject literature we can now find several tens of empirical light absorption spectra of structurally pure liquid water (redistilled

TABLE 2.11. Light attenuation coefficient c_w and light absorption coefficients a_w in distilled water; light absorption coefficients a in pure natural waters.

Type of water	Distilled	Distilled	Distilled	Distilled	Distilled	Pure natural waters	Sargasso sea	Central pacific
Source	Clarke, James (1939)	Clarke, James (1939), Le Grand (1939)[a]	Shuleykin (1959)	Hale, Querry (1973)	Morel, Prieur (1977)	Smolu-chowski (1908)	Ivanov (1975)	Pelevin, Rostovt-seva (2001)
	Measured Parameter							
λ [nm]	c_w [m^{-1}]	a_w [m^{-1}]	a_w [m^{-1}]	a_w [m^{-1}]	a_w [m^{-1}]	a [m^{-1}]	a [m^{-1}]	a [m^{-1}]
-1-	*-2-*	*-3-*	*-4-*	*-5-*	*-6-*	*-7-*	*-8-*	*-9-*
375	0.045	0.0383	—	0.117	—	—	—	
390	—	—	—	—	0.020	0.038	0.041	0.012
400	0.043	0.0379	—	0.056	0.018	—	—	0.012
410	—	—	—	—	0.018	0.037	0.034	0.011
425	0.033	0.0291	—	0.038	—	—	—	—
430	—	—	—	—	0.015	0.036	0.025	0.011
450	0.019	0.0159	—	0.028	0.015	0.037	0.016	0.012
470	—	—	—	—	0.016	0.039	0.014	0.012
475	0.018	0.0155	—	0.025	—	—	—	—
490	—	—	—	—	0.020	0.042	0.018	0.017
494	—	—	0.002	—	—	—	—	—
500	0.036	0.0340	—	0.025	0.026	—	—	0.019
510	—	—	—	—	0.036	0.054	0.023	0.026
522	—	—	0.002	—	—	—	—	—
525	0.041	0.0394	—	0.032	—	—	—	—
530	—	—	—	—	0.051	0.062	0.039	0.038
550	0.069	0.0676	—	0.045	0.064	0.074	0.05	0.052
558	—	—	0.038	—	—	—	—	—
570	—	—	—	—	0.080	0.094	0.067	0.075
575	0.091	0.0898	—	0.079	—	—	—	—
590	—	—	0.089	—	0.157	0.160	0.140	0.121
600	0.186	0.1850	—	0.230	0.244	—	—	0.162
602	—	—	0.173	—	—	—	—	—
607	—	—	0.200	—	—	—	—	—
610	—	—	—	—	0.289	0.260	0.240	—
612	—	—	0.233	—	—	—	—	—
617	—	—	0.234	—	—	—	—	—
622	—	—	0.239	—	—	—	—	—
625	0.228	0.2272	—	0.280	—	—	—	—
643	—	—	0.291	—	—	—	—	—
650	0.288	0.2873	—	0.320	0.3492	0.380	0.330	—
658	—	—	0.320	—	—	—	—	—
675	0.367	0.3664	—	0.415	—	—	—	—
690	—	—	—	—	0.5	0.540	0.520	—
700	0.500	0.4995	—	0.600	0.6499	—	—	—

[a] Values calculated as the difference $a_w = c_w - b_w$, where c_w is the light attenuation coefficient of pure water (after Clarke and James (1939)); b_w is the light scattering coefficient of pure water (after Le Grand (1939)).

water) or of pure natural waters (i.e., practically devoid of admixtures) meticulously plotted for a variety of spectral ranges (see the introduction to Section 2.2). Some of these empirical spectra of $a_w(\lambda)$ are compared in Figure 2.12. The plots in Figure 2.12a show such spectra of $a_w(\lambda)$ for a wide

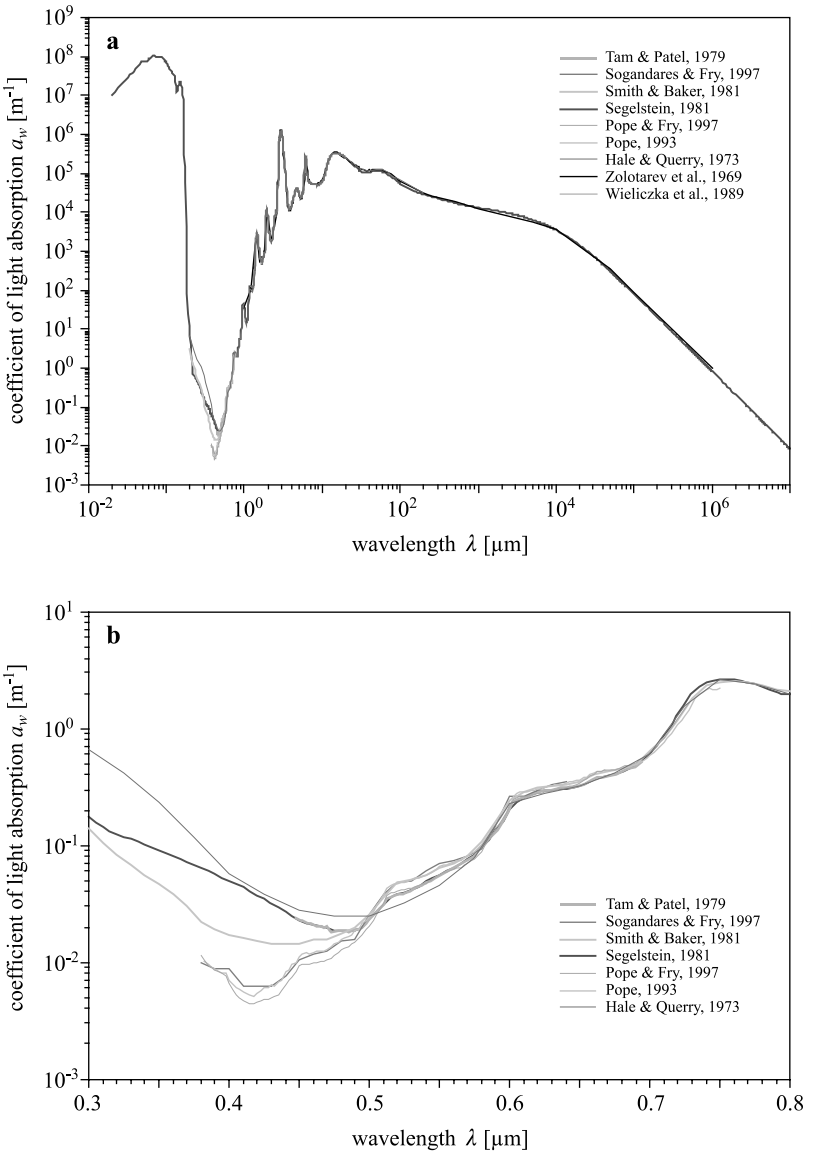

FIGURE 2.12. Empirical absorption spectra of liquid water, as determined by various authors: (a) in the wide spectral range from the ultraviolet to short radiowaves; (b) in the visible range and its nearest neighborhood. (See Colour Plate 2)

spectral range (from UV light to microwave and short radiowave radiation), and those in Figure 2.12b illustrate the spectra in the VIS region and its nearest neighborhood. Table 2.11, moreover, sets out some of these measurements in the visible part of the spectrum of $a_w(\lambda)$ in distilled water and in pure natural waters, whereas Table 2.12 gives examples (from Hale and Querry (1973)) of IR absorption coefficients $a_w(\lambda)$ of pure water.

We can see from the plots in Figure 2.12 and the data in Table 2.11 that there are discrepancies among the empirical absorption spectra of $a_w(\lambda)$ of liquid water obtained by various authors. With respect to those regions of the spectrum with high absorption coefficients (i.e., UV, IR, and longer waves; see Figure 2.12a), these discrepancies are small and can be neglected. But as far as visible and near-UV light is concerned, they are very significant and

TABLE 2.12. IR absorption coefficients $a_w(\lambda)$ in pure liquid water.

λ [μm]	a [m^{-1}]	λ [μm]	a [10^3 m^{-1}]	λ [μm]	a [10^3 m^{-1}]
-1-	*-2-*	*-1-*	*-2-*	*-1-*	*-2-*
0.70	0.60	1.40	1.23	4.00	14
0.725	1.59	1.60	0.067	4.10	17
0.75	2.60	1.80	0.802	4.20	21
0.775	2.40	2.00	6.91	4.30	25
0.80	2.00	2.20	16.5	4.40	29
0.81	1.99	2.40	50.05	4.50	37
0.82	2.39	2.60	15.32	4.60	40
0.83	2.91	2.65	31.77	4.70	42
0.84	3.47	2.70	88.4	4.80	39
0.85	4.30	2.75	269.6	4.90	35
0.86	4.68	2.80	516	5.00	31
0.87	5.20	2.85	815	5.10	28
0.875	5.60	2.90	1161	5.20	24
0.88	5.60	2.95	1269	5.30	23
0.89	6.04	3.00	1139	5.40	24
0.90	6.80	3.05	988	5.50	27
0.91	7.29	3.10	778	5.60	32
0.92	10.93	3.15	538	5.70	45
0.93	17.30	3.20	363	5.80	71
0.94	26.74	3.25	236	5.90	132
0.95	39.0	3.30	140	6.00	224
0.96	42.0	3.35	98	6.10	270
0.97	45.0	3.40	72	6.20	178
0.98	43.0	3.45	48	6.30	114
0.99	41.0	3.50	34	6.40	88
1.00	36.0	3.60	18	6.50	60
1.10	17.0	3.70	12	6.60	68
1.20	104	3.80	11	6.70	63
1.30	111	3.90	12	6.80	60

Selected from data published by Hale and Querry (1973).

cannot be ignored (Figure 2.12b). This applies both to the absolute values and to the position of the minimum of coefficient $a_w(\lambda)$ in the spectrum. These discrepancies are due primarily to the difficulties, mentioned earlier, in obtaining chemically (and therefore spectrally) pure water, free of all admixtures, especially of suspended particulate matter.

Regardless of these differences in the spectral dependences of light absorption on wavelength, all the empirical spectra of $a_w(\lambda)$, determined empirically by various authors, confirm the existence of a deep minimum of absorption intensity in the blue light area, probably at c. $\lambda_{\min} \approx 415$ nm. A much trickier problem, however, is to discover which of these empirical results are characterized by absolute values of $a_w(\lambda)$ most closely approaching the real values in the visible and near-UV regions. As yet there is no definitive solution. What we can state with a fair degree of certainty, though, is that they may very well be the figures quoted in Table 2.13 for various light wavelengths in the 200 nm $< \lambda <$ 700 nm range. The absorption coefficients $a_w(\lambda)$ given in this table for various spectral subranges were gleaned from a number of works (see the footnotes to this table; Smith and Baker (1981), Sogandares and Fry (1997), and Pope and Fry (1997)). We should add that among the dozen or so most reliable light absorption spectra of water for this spectral region that we analyzed, these values are intermediate. The spectra of $a_w(\lambda)$ quoted in Table 2.13 can therefore be applied with confidence in practical model calculations[14] (see, e.g., Woźniak et al. (2005b[15])).

Finally, it is worth pointing out that, as Table 2.11 shows, the waters of pure natural bodies (some mountain lakes, such as Crater Lake in the United States), and also saline but pure areas of the ocean (e.g., the Sargasso Sea), absorb visible light in practically the same way as distilled water does, except for some subtle differences in the UV band. Some authors, for example, Pelevin and Rostovtseva (2001), would go further: they consider that these absorption coefficients of pure natural water bodies, determined in situ, most closely approach the real absorption coefficients of this light in structurally pure water. Their argument in support of this claim is that the accuracy of in vitro measurements in pure redistilled water is worse than that of in situ measurements, because of the small optical pathways obtainable in laboratory spectrophotometers.

---

[14] As far as the values of the coefficients $a_w(\lambda)$ from the IR region are concerned, we can use the data of, for example, Hale and Querry (1973) given in Table 2.12 in such model calculations to good effect. This is because the values of these coefficients given by other authors are similar.

[15] All tables and graphs taken for this book from the journal *Oceanologia* are reproduced with the kind permission of the Polish Academy of Sciences Institute of Oceanology and the National Committee on Oceanic Research.

TABLE 2.13. Spectral light absorption coefficients of liquid water in the 200–700 nm region suggested in this monograph.[a]

Light wavelength [nm]	a_w [m^{-1}]	Light wavelength [nm]	a_w [m^{-1}]	Light wavelength [nm]	a_w [m^{-1}]
-1-	*-2-*	*-1-*	*-2-*	*-1-*	*-2-*
200	3.070	370	0.0114	540	0.0474
205	2.530	375	0.0114	545	0.0511
210	1.990	380	0.0114	550	0.0565
215	1.650	385	0.0094	555	0.0596
220	1.310	390	0.0085	560	0.0619
225	1.120	395	0.0081	565	0.0642
230	0.930	400	0.0066	570	0.0695
235	0.820	405	0.0053	575	0.0772
240	0.720	410	0.0047	580	0.0896
245	0.640	415	0.0044	585	0.1100
250	0.559	420	0.0045	590	0.135
255	0.508	425	0.0048	595	0.167
260	0.457	430	0.0050	600	0.222
265	0.415	435	0.0053	605	0.258
270	0.373	440	0.0064	610	0.264
275	0.331	445	0.0075	615	0.268
280	0.288	450	0.0092	620	0.276
285	0.252	455	0.0096	625	0.283
290	0.215	460	0.0098	630	0.292
295	0.178	465	0.0101	635	0.301
300	0.141	470	0.0106	640	0.311
305	0.123	475	0.0114	645	0.325
310	0.105	480	0.0127	650	0.340
315	0.0947	485	0.0136	655	0.371
320	0.0844	490	0.0150	660	0.410
325	0.0761	495	0.0173	665	0.429
330	0.0678	500	0.0204	670	0.439
335	0.0620	505	0.0256	675	0.448
340	0.0325	510	0.0325	680	0.465
345	0.0265	515	0.0396	685	0.486
350	0.0204	520	0.0409	690	0.516
355	0.0180	525	0.0417	695	0.559
360	0.0156	530	0.0434	700	0.624
365	0.0135	535	0.0452		

Data from various authors, after Woźniak et al. (2005b).

[a] Values assumed on the basis of data from various authors and linearly approximated: in the 200–335 nm range, after Smith and Baker (1981); 340–370 nm, after Sogandares and Fry (1997); 380–700 nm, after Pope and Fry (1997).

The Absorption of Electromagnetic Radiation by Water: Its Influence on the Biological Evolution of Life

To conclude this chapter, we draw the reader's attention to the perfect adaptation of life on our planet to, among other things, the optical properties of water and to the most important features of solar radiation. Let us therefore take a look at the plots in Figure 2.13. They illustrate the dependence on

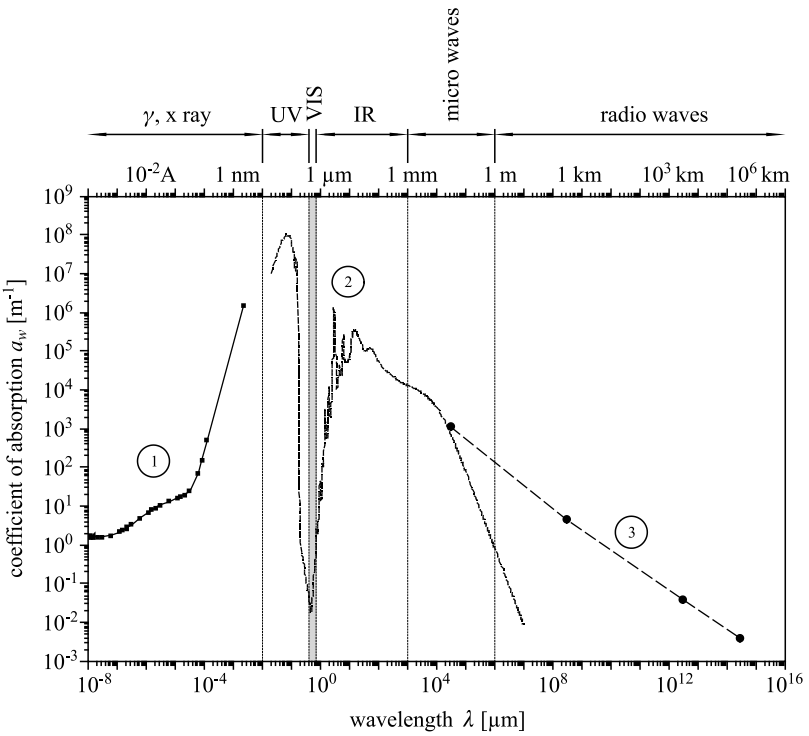

FIGURE 2.13. Electromagnetic waves absorption spectra of liquid water over the complete spectral range, from high-energy quanta γ ($\lambda \approx 10^{-4}$ Å) to long radio waves ($\lambda \approx 3 \times 10^5$ km). (1) Relationship among the radiation absorption coefficient of pure water and the wavelength for γ-radiation, X-radiation, and high-energy UV photons (based on data from Aglintzev (1961/1957), Jaeger (1962/1959), Ciborowski (1962), Adamczewski (1965), and others); (2) same relationship for pure water in the UV-short radiowave range (after Segelstein (1981)); (3) the same relationship for oceanic salt water in the microwave-longwave ($\lambda \approx 3 \times 10^5$ km) region determined approximately on the basis of data from Popov et al. (1979).

wavelength of the light absorption coefficients of water over their entire range, almost 11 orders of magnitude. The wavelengths we have taken into consideration here embrace the even greater range of more than 22 orders of magnitude, from short γ-radiation (c. 10^{-4} A) to extremely long radiowaves (c. 300,000 km), in other words, practically the entire range of electromagnetic radiation existing in Nature. First, the figure shows the spectrum of absorption in water of γ-, X-, and very-high-energy UV radiation. This absorption is due to interaction between the high-energy photons of this radiation and the inner electrons of the oxygen atom and the hydrogen and oxygen nuclei (plot 1 in Figure 2.13).

Next, plot 2 in this figure represents the spectrum of absorption in the UV-short-radiowave range, that is, absorption caused by standard electronic, vibrational (including librations and cluster vibrations), and rotational transitions, and also dipole-electric field interactions. Finally, plot 3 shows the spectrum of the absorption in saline oceanic water of radio waves (also very long). Such water absorbs these waves with greater intensity, an intensity that is all the more suited to the conditions prevailing on our planet inasmuch as the resources of salt water in the oceans are very much greater than the Earth's supplies of fresh water.

Figure 2.13 shows, therefore, that water—natural, omnipresent, and indispensable to life on Earth—is opaque to most electromagnetic radiation and is characterized by just the one deep spectral "window" for the transmission of radiation (of low absorption), in the visible light spectral range.[16] At the same time, we know that the maximum solar emission falls within this window, and that some 50% of the solar radiation reaching the Earth's surface lies within the VIS range. Is it surprising, then, that biological evolution on our planet, full of water as it is, has brought into existence plants that are green in color[17] (including marine phytoplankton), drawing their vital energy from the solar radiation flowing in through this window, and on the other hand, has caused animals to develop eyes with which they can perceive light, from red to violet, which readily penetrates the water? Mother Nature has undoubtedly made excellent use of her window. You, the reader, may wonder at this point: is this purely coincidence, or is it design?

2.2.3 The Absorption of Electromagnetic Radiation in Ice

As ice forms, all the water molecules (in the case of monocrystalline ice) or the vast majority of them (in the case of polycrystalline or amorphous ice) become attached to their neighbors, mostly by means of hydrogen bonds. As a result of these intermolecular interactions many possible geometrical structures of ice, both crystalline and amorphous, can come into and remain in existence. This depends on the thermodynamic conditions (temperature and pressure) prevailing during the formation of ice and while it lasts. The contemporary literature on the physics of ice describes some 20 possible

---

[16] Absorptions as low as those in the VIS region are only again attainable in the region of radiowaves thousands of kilometers long (in the case of sea water). Such low absorption is also conceivable with respect to shortwave radiation in the $\lambda < 10^{-4}$ A region, that is, for neutrino radiation.

[17] The green color of plants is, as we know, due to the absorption properties of chlorophyll and the other pigments essential to the photosynthesis of organic matter in plants. We return to these questions in Chapter 6.

geometrical structures of ice[18] (Hobbs (1974), Eisenberg and Kauzmann (1969), Chaplin (2006), and the papers cited therein). These structures differ not only in their geometry, but also in a number of physical properties, including such fundamental ones as density, the value of which can be from 0.92 (types Ih and Ic) to 2.51 (type X) and more (type XIII) times the density of liquid water under natural conditions.

They also differ considerably in their relative permittivity ε (dielectric constant; Table 2.1, item 8), one of the basic electromagnetic properties governing the interaction of a material with electromagnetic radiation. The relative permittivity ε for liquid water under normal conditions is c. 78.4; for the different types of ice it varies widely: from small values of c. 3.74 for type IX ice, through intermediate values of c. 97.5 for the common type Ih ice, up to the very high value of c. 193 for type VI ice (Chaplin 2006, Robinson et al. 1996).

In view of this, the optical properties of these different structural forms of ice, and their absorption capacities in particular, will vary widely as well (Warren (1984) and the papers cited therein). We do not deal with these problems here, because with the exception of type Ih ice, which occurs naturally all over the Earth, most of the other structures of ice do not occur in the sea or the atmosphere. They form only at the extremely high pressures produced in laboratories for experimental purposes.

An exception is type Ic ice, which forms under natural conditions in tropical cirrus clouds (Warren 1984); its absorption properties approach those of type Ih. That is why we limit our description of the absorption properties of ice to the monocrystals of type Ih ice, and primarily its polycrystalline forms (more easily obtainable), which consist of single crystals c. 0.1 cm in diameter. Studies have shown that the absorption properties of this polycrystalline ice are practically identical to those of an ice monocrystal (Hobbs 1974). The pure form of this ice has a density of c. 920 kg m^{-3} and comes into existence under natural conditions when distilled water, free of air bubbles and other particulate admixtures, freezes. In these conditions, water crystallizes into the hexagonal arrangement of tetrahedral unit cells characteristic of type Ih ice. Such an ice monocrystal is birefringent and uniaxial, with the optical axis coinciding with the crystallographic c-axis. The reader can find more detailed information on the structures of hexagonal type Ih ice and its fundamental properties in Eisenberg and Kauzmann

[18] Among them are the following crystalline and noncrystalline structures: hexagonal with density (expressed in g cm^{-3}) equal to $\rho = 0.92$, type Ih; cubic with $\rho = 0.92$, type Ic; noncrystalline with $\rho = 0.94$, LDA-type (low-density amorphous ice); noncrystalline with $\rho = 1.17$, HDA-type (high-density amorphous ice); noncrystalline with $\rho = 1.25$, VHDA-type (very high-density amorphous ice); rhombohedral with $\rho = 1.17$, type II; tetragonal with $\rho = 1.14$, type III; rhombohedral with $\rho = 1.27$, type IV; monoclinic with $\rho = 1.23$, type V; tetragonal with $\rho = 1.46$, type VIII; tetragonal with $\rho = 1.16$, type IX; cubic with $\rho = 2.51$, type X; orthorhombic with $\rho = 0.92$, type XI; tetragonal with $\rho = 1.29$, type XII; and hexagonal with $\rho > 0.92$, type XIII.

(1969), Hobbs (1974), Doronin and Chieysin (1975), Soper (2000), and Robinson et al. (1996).

In the first part of this section we characterize the principal spectral features of radiation absorption in pure type Ih ice. We also review the empirical absorption spectra of ice determined by various authors. The reader should bear in mind that natural ice forming in seas and in freshwater basins often has optical properties that deviate from those of the well-researched pure type Ih ice, which is usually obtained in the laboratory. We discuss the reasons for these discrepancies in the optical properties of natural and pure ice in the last part of this section.

The Absorption of Radiation in Pure Ice: Principal Spectral Features

The absorption spectrum of pure crystalline ice $a_{w,ice}(\lambda)$ in the near-UV-short radiowave range is illustrated in Figure 2.14; for comparison, this also

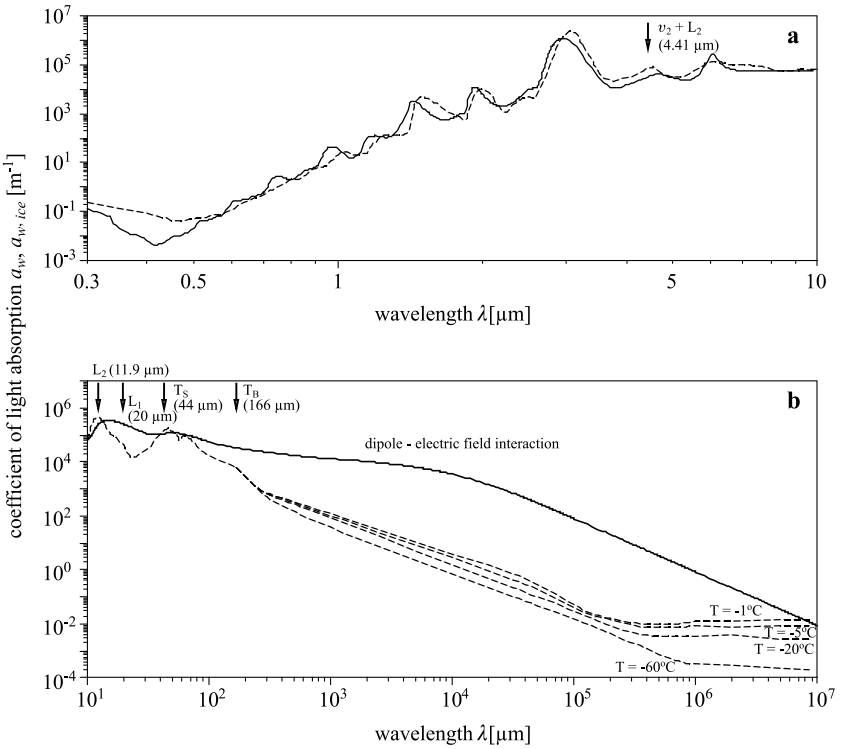

FIGURE 2.14. Visible light – short radio wave absorption spectra of liquid water and ice. The positions of the absorption band peaks due to librations and transitional vibrations are indicated, as is the area of "dipole-electric field interaction" in the ice crystal (denotations as in Figure 2.11). Dashed lines – ice (Warren 1984), Continuous lines – liquid water : 0.3 – 0.7 μm (Woźniak et al. 2005b), 0.7 – 10^7 μm (Segelstein 1981).

shows the corresponding absorption spectrum of pure water $a_w(\lambda)$. Because of intermolecular interactions, the spectra of both $a_{w,ice}(\lambda)$ and $a_w(\lambda)$ are continuous across the whole spectral range in question, which is not the case with the spectra of free molecules or water vapor. The absorptions of radiation in ice and liquid water have numerous spectral features in common, but there are also a number of features differentiating the absorption spectra in these two media. We discuss these features with respect to the following three spectral ranges: (1) UV, VIS, and near-IR light from $\lambda < 2.5$ μm, (2) intermediate IR in the $2.5 < \lambda < 8$ μm range, and (3) longwave radiation from $\lambda > 8$ μm.

In range (1) (UV–VIS–near-IR as far as λ = c. 2.5 μm) of the absorption spectrum of $a_{w,ice}(\lambda)$, as in the case of liquid water, there is a whole series of broadened and overlapping absorption bands, decreasing in intensity with shortening wavelength (see the left-hand side of Figure 2.14a; also Table 2.9, items 11–18). In the blue part of the VIS region there is an absolute minimum of absorption $a_{w,ice}(\lambda)$ in the spectrum of ice, as in the corresponding spectrum of liquid water. In comparison with the latter, however, the ice minimum is shifted slightly towards the longer waves and is located at $\lambda \approx 475$ nm. (The position of the liquid water minimum is at $\lambda \approx 415$ nm.) The increase in absorption coefficients on the shortwave side of these minima in the spectra of both $a_{w,ice}(\lambda)$ and $a_w(\lambda)$ is caused by absorption due to electronic transitions, whereas all the absorption bands on the longwave side are vibrational-rotational. The UV absorption spectrum of ice resembles that of liquid water (part of the UV region is visible in Figure 2.14). Should the reader wish for a more detailed account of this absorption, we refer him or her to the relevant literature: Daniels (1971), Browell and Anderson (1975), Seki et al. (1981), and Warren (1984).

The absorption bands on the longwave side of the absorption minimum in the spectra of $a_{w,ice}(\lambda)$ and $a_w(\lambda)$ in the VIS and near-IR regions correspond to vibrational-rotational transitions, as in the case of free molecules. In this spectral region they are combination and higher harmonic transitions from the ground state to excited state, exactly the same as for free molecules (Figure 2.3a). In comparison with the liquid water bands, the ice bands are shifted towards the longer wavelengths, in the same way as the absorption minimum, mentioned above. Moreover, the outline of these bands in the absorption spectrum of ice, and also all their irregularities, especially in the shortwave part of the spectral region in question, are expressed less distinctly than in the spectrum of liquid water. As a result, these three weak although discernible absorption bands, characteristic of liquid water in the wavelength ranges c. $510 < \lambda < 560$ nm, $600 < \lambda < 680$ nm, and $700 < \lambda < 800$ nm, are scarcely perceptible in the spectrum of ice.

Notice also that the absolute absorption coefficients in the longwave part of the spectral range $\lambda < 2.5$ μm are similar for ice and liquid water, if we ignore the shifts of the separate absorption bands. Only in the shortwave VIS range ($\lambda < 570$ nm) are these coefficients markedly larger than for liquid

water. In the 350–450 nm range, the borderland between VIS and UV light, this difference is about one order of magnitude. This means that in this spectral range pure ice is much less transparent than pure liquid water.

Range (2) (intermediate IR; $2.5 < \lambda < 8$ μm) is characterized by the presence of "pure" fundamental vibrational-rotational absorption bands, or their combination with librations (see the right-hand side of Figure 2.14a and Table 2.9, items 6–10) against a background of an absorption continuum, as in the case of liquid water. These bands peak at $\lambda = 3.08$ μm, 4.41 μm, and 6.06 μm. The first of these, the absorption band in the vicinity of $\lambda = 3.08$ μm, is the strongest absorption band in the range of wavelengths longer than those of VIS light. It corresponds to band X of water vapor and is formed jointly by fundamental mode I and mode III transitions. The second band, with a maximum at c. $\lambda = 4.41$ μm, is a combination band of bending (υ_2) and librations (mode L_2), and the third one, peaking at c. $\lambda = 6.06$ μm, is due to frequent bending (υ_2), that is, mode II transitions.

Figure 2.14a shows that these principal absorption bands of ice closely resemble the analogous absorption bands of liquid water in that their peak positions, intensities, and breadths are all similar. The last-mentioned band (peaking at c. $\lambda = 6.06$ μm), however, is an exception: although somewhat less clearly expressed than its counterpart in the liquid water spectrum (peaking at $\lambda = 6.08$ μm), it is much broader. Nonetheless, the absorption spectra of liquid water $a_w(\lambda)$ and of ice $a_{w,ice}(\lambda)$ coincide most closely in this wavelength range (2.5–8 μm), certainly more so than in other spectral ranges.

Finally, range (3) (far-IR, microwaves, and radio waves; $\lambda > 8$ μm) exhibits the greatest differences between the spectra of water $a_w(\lambda)$ and of ice $a_{w,ice}(\lambda)$ (Figure 2.14b; Table 2.9 items 1–5). In comparison with the absorption coefficients of liquid water, those of ice in this range are usually from one to three orders of magnitude smaller. Exceptional in this respect are two narrower intervals in the IR region, where these coefficients for ice and water are similar (see the left-hand side of the plot in Figure 2.14b). As in the case of liquid water, we find here the L_1(20 μm) and L_2(11.9 μm) libration bands, as well as the T_S(44 μm) and T_B(166 μm) cluster vibration bands, characteristic of both condensed phases. But in the case of ice these bands are expressed much more distinctly than in the case of liquid water, and they are also shifted a little towards the shorter wavelengths. This is in part due to the fact that in ice, these bands overlap absorption bands due to molecular vibrations in the crystal lattice, which, of course, are characteristic only of the solid state (see Section 2.2.1).

In the UV, VIS, and IR regions, the absorption coefficient of ice varies only slightly with temperature changes between c. 0 and –30°C. Only when the temperature drops below –40°C does it begin to have a marked effect on the absorption coefficient of ice. On the other hand, where longer wavelengths are concerned (microwaves and radiowaves; $\lambda > 250$ μm), the

absorption coefficient is significantly affected at all subzero temperatures (see the middle and right-hand parts of the plot in Figure 2.14b) in that the absorption intensity falls sharply as the temperature of the ice drops (Jiracek 1967, Johari et al. 1975, Warren 1984). Thus, in the radiowave range $\lambda = 10^6$–10^7 μm, the difference between the absorption coefficients of ice at around freezing point (0°C) and at −60°C is almost two orders of magnitude.

Empirical Light Absorption Spectra of Ice: A Review

The light absorption spectra of ice, like those of water, have been determined empirically by several dozen authors (see the introduction to Section 2.2), but in most cases within strictly limited spectral ranges. In a synthesis of all this work, Warren (1984) presented spectra of the real and imaginary part of refractive indices over a wide spectral range from UV (44.3 nm) to radiowaves (8.6 m) and at different temperatures from −1°C to −60°C. The spectrum of the absorption coefficient of ice[19] $a_{w,ice}(\lambda)$ plotted from these data is illustrated in Figure 2.15 (selected values of $a_{w,ice}$ for the spectral range from 195 nm to 6.75 μm are given in Table 2.14). The figure also shows, for comparison, three such empirical spectra postulated by other authors for somewhat narrower spectral ranges.

Hence, there are discrepancies also in the empirical spectra of $a_{w,ice}(\lambda)$ determined by various authors: they are marked in the VIS region and its nearest neighborhood, that is, in the range where absorption coefficients are very low. The reasons for this are the same as in the case of liquid water, namely, the difficulties of obtaining sufficiently pure ice, and technical imperfections on the other hand. It is thus hard to state definitively which of the absorption coefficients $a_{w,ice}(\lambda)$ in the spectra plotted in Figure 2.15 are closest to the real values in and around the VIS region. It does seem, however, that these coefficients in other spectral regions are encumbered with smaller errors.

Reasons for Discrepancies Between the Optical Properties of Natural and Pure Ice

The natural ice that forms on the surface of fresh- and salt-water bodies is a multicomponent substance, the properties of which differ from those of ice monocrystals (type Ih), or the similar polycrystalline ice produced artificially

[19] If the relevant coefficients of the imaginary part of refractive indices are known, light absorption coefficients can be calculated from the relationship $a = 4\pi n'/\lambda$, where n' is the coefficient of the imaginary part of the refractive index of light, called for short the imaginary refractive index (see Chapter 5).

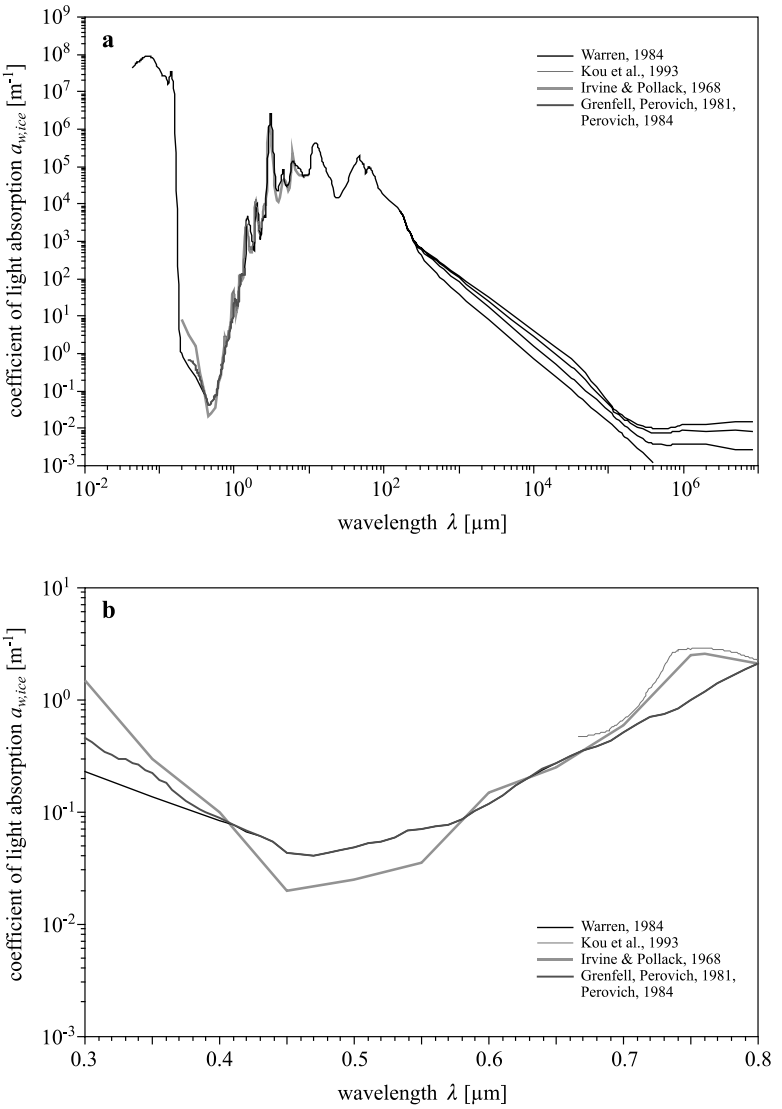

FIGURE 2.15. Empirical radiation absorption spectra of ice, as determined by various authors: (a) in the wide spectral range from the ultraviolet to short radio waves; (b) in the visible range and its nearest neighborhood. (See Colour Plate 3)

from distilled water or pure optically natural water and consisting predominantly of crystals c. 1 mm across.

The size and forms of the crystals constituting natural ice on bodies of open water depend on the degree of supercooling of the water, the rate of heat loss during crystallization, the rate of crystal nucleation, the salinity of the water,

TABLE 2.14. Light absorption coefficients $a_{w,ice}$ of type Ih ice; spectral range from 195 nm to 6.75 μm.

λ [μm]	a [m^{-1}]	λ [μm]	a [m^{-1}]	λ [μm]	a [m^{-1}]
-1-	*-2-*	*-1-*	*-2-*	*-1-*	*-2-*
0.195	1.025	0.660	0.316	2.350	2.93×10^3
0.210	0.793	0.670	0.354	2.500	4.65×10^3
0.250	0.433	0.680	0.386	2.565	4.26×10^3
0.300	0.231	0.690	0.437	2.600	4.88×10^3
0.350	0.135	0.700	0.521	2.817	1.70×10^5
0.400	0.085	0.710	0.609	3.003	1.83×10^6
0.410	0.077	0.720	0.703	3.077	2.55×10^6
0.420	0.068	0.730	0.740	3.115	2.17×10^6
0.430	0.061	0.740	0.835	3.155	1.74×10^6
0.440	0.055	0.750	0.984	3.300	3.92×10^5
0.450	0.043	0.760	1.171	3.484	6.71×10^4
0.460	0.042	0.770	1.400	3.559	3.74×10^4
0.470	0.041	0.780	1.643	3.775	2.20×10^4
0.480	0.043	0.790	1.877	4.099	3.40×10^4
0.490	0.046	0.800	2.105	4.239	4.30×10^4
0.500	0.048	0.820	2.191	4.444	7.35×10^4
0.510	0.053	0.850	2.705	4.56	8.27×10^4
0.520	0.055	0.910	6.131	4.904	3.31×10^4
0.530	0.060	0.970	1.20×10^1	5.000	3.02×10^4
0.540	0.068	1.030	2.84×10^1	5.100	3.08×10^4
0.550	0.071	1.100	1.94×10^1	5.263	3.34×10^4
0.560	0.074	1.180	5.08×10^1	5.556	5.43×10^4
0.570	0.078	1.270	1.34×10^2	5.747	8.31×10^4
0.580	0.088	1.310	1.26×10^2	5.848	1.12×10^5
0.590	0.104	1.40	1.78×10^2	6.061	1.43×10^5
0.600	0.12	1.504	4.93×10^3	6.135	1.43×10^5
0.610	0.142	1.587	2.93×10^3	6.250	1.35×10^5
0.620	0.174	1.850	5.45×10^2	6.369	1.22×10^5
0.630	0.207	2.000	9.98×10^3	6.452	1.11×10^5
0.640	0.24	2.105	5.02×10^3	6.579	1.05×10^5
0.650	0.276	2.245	1.13×10	6.757	1.08×10^5

Data selected from Warren (1984).

and also on the degree of wind-mixing of the water. This last factor applies to the surface layer of ice (Doronin and Chieysin 1975, Hobbs 1974). Strong supercooling and a slow rate of heat loss favor the formation of skeletal crystals, whereas the opposite situation—weak super cooling and a rapid loss of heat—promotes the formation of compact crystals. The subject literature distinguishes black and white ice. The former arises directly from water as this freezes, the latter when ice remelts together with rainwater, with water from melting ice, or water flowing over the surface of ice when this is melting, for example, under the weight of snow. Repeated melting and freezing of the surface layer of an ice covering causes this layer to become grainy and inhomogeneous, regardless of its original structure (Hobbs 1974, Grenfell 1991). The physical properties of such white ice therefore differ from those of black ice.

Furthermore, natural sea ice, because of the dynamically changing conditions of crystallization, is inhomogeneous and consists of alternate layers or patches of white and black ice. Apart from crystals of pure ice, sea ice also incorporates salt, gas bubbles, and other admixtures present in sea water (Grenfell and Maykut 1977, Zakrzewski 1982, Light et al. 2004).

These factors are the reason why the absorption of electromagnetic radiation in natural sea ice is a complex phenomenon. The radiation penetrating the surface of such ice is absorbed by both the ice crystals and by the admixtures contained in the ice; not only that, it is also scattered, and this scattering is generally stronger than the absorption (Perovich 1990, Grenfell 1991). The intensity of scattering in sea ice depends principally on its content of brine cells and capillaries (water that has become strongly saline as a result of the precipitation of salts during freezing) and of micropores remaining after the brine and the solid admixtures have trickled out (Grenfell and Hedrick 1983).

The light scattering at these constituents of the ice can be treated as the reflection and refraction of light at the successive interfaces of an inhomogeneous medium. As a result, the passage of light through a layer of ice is a process specific to ice, in which the resultant attenuation of the light by the ice depends on the number and orientation of the refracting surfaces, and also the refractive indices and absorption properties of the constituents of the ice (ice crystals, brine, air, solid admixtures). This is why it is difficult to define experimentally the spectral absorption coefficients of natural ice. In descriptions of the transmission of electromagnetic waves through a layer of natural ice, therefore, it is usual to employ the coefficient of irradiance transmission or the albedo of the ice. The reader can find detailed data on the value of these coefficients for sea ice from various parts of the Arctic and Antarctic in Grenfell and Maykut (1977), Grenfell and Perovich (1984), Perovich et al. (1986), Perovich (1994), and Hanesiak et al. (2001). The magnitudes of these coefficients, and also the influence of marine environmental parameters and the structural properties of sea ice on its optical properties and on radiation transfer in sea ice have recently been the subject of mathematical modeling (see, e.g., Mobley et al. (1998), Light et al. (2003, 2004), and the papers cited therein).

Snow is far less transparent to visible light than ice. This effect is due primarily to the structure of snow, which consists of ice grains interspersed with air. This causes light to be strongly scattered as a result of multiple reflections, whereby the degree of scattering is so large that the transport of radiant energy through snow can be treated as a diffusion process. As a consequence of this property, a 3 cm thick covering of snow on a surface of ice is enough to practically prevent any transmission of light through that ice. The optical properties of snow are described by Grenfell and Maykut (1977), Grenfell and Perovich (1986), Grenfell (1991), Perovich et al. (1986), and Warren (1984), among others.

2.3 Light Absorption by Atoms, Sea-Salt Ions, and Other Inorganic Substances Dissolved in Sea Water

Practically all natural elements are present in the World Ocean, although most of them in very low concentrations (e.g., Dera (2003)). They occur mostly as dissolved forms of inorganic and organic matter. The inorganic forms are represented not only by atoms and simple ions, but also by molecules and complex ions. Changes in the electronic states of the atoms and ions of the various elements (see Table 2.15) give rise to a narrow absorption band at the shortwave end of the electromagnetic spectrum, beginning with the visible region (and sometimes with the near-IR).

Radiation is absorbed by the atoms and ions of these elements as a result of the excitation of the weakly bound electrons in their unfilled *d* orbitals (e.g., Gołębiewski (1982), McQuarrie (1983), and Love and Peterson (2005)). The atoms and ions of elements with other configurations usually need higher excitation energies for absorption to occur—their absorption bands are located in the far ultraviolet—for instance, the chloride ion Cl^- absorbs radiation with a wavelength of 181 nm. These features of the absorption of radiation by inorganic substances, that is, the narrow absorption bands for the individual elements, although present in sea water, are scarcely detectable against the background of the total absorption of all the dissolved substances.[20]

The first empirical studies on the influence of all the inorganic substances dissolved in sea water on its optical properties (Hulburt 1928) showed that they strongly attenuated and absorbed UV and VIS radiation.

TABLE 2.15. The area of spectrally active elements in the periodic table.[a]

H																	He
Li	Be											B	C	N	O	F	Ne
Na	Mg											Al	Si	P	S	Cl	Ar
K	Ca	Sc	**Ti**	**V**	**Cr**	**Mn**	**Fe**	**Co**	**Ni**	**Cu**	Zn	Ga	Ge	As	Se	Br	Kr
Rb	Sr	Y	**Zr**	**Nb**	**Mo**	**Tc**	**Ru**	**Rh**	**Pd**	Ag	Cd	In	Sn	Sb	Te	I	Xe
Ca	Ba	La	Hf	**Ta**	**W**	**Re**	**Os**	**Ir**	**Pt**	**Au**	Hg	Ti	Pb	Bi	Po	At	Rn
Fr	Ra	Ac															

[a] The lanthanides and actinides have been omitted. The elements whose atoms and ions absorb visible and near-UV radiation (>300 nm) are highlighted in bold; the other elements absorb radiation in the far-UV region.

[20] Exceptional are the fairly narrow bands due to the absorption of radiation by metal ion complexes (Kondratev and Pozdniakov 1988), which can occur in the absorption spectra of waters mineralized to a high degree, for example, certain lakes; see the section 2.3.3 on inorganic complexes below.

These results were, however, overestimated as a result of methodological errors (contaminated water samples). Later work, for example, that by Clarke and James (1939) and by Sullivan (1963), indicated that the effect of inorganic substances on visible light absorption was so small as to be practically negligible. It is important to note, however, weak bands due to the absorption by inorganic substances of IR radiation were found (e.g., Visser (1967)), and the absorption of UV radiation by these substances in sea water was quite considerable in comparison to its absorption in pure water (e.g., Lenoble (1956) and Armstrong and Boalch (1961)). Nevertheless, these results were of a qualitative nature. In the light of subsequent research (see below) it has become possible to perform quantitative analyses, and in some cases to distinguish the elements and inorganic compounds responsible for certain spectral properties of sea water (Table 2.15 and Figure 2.16). Our

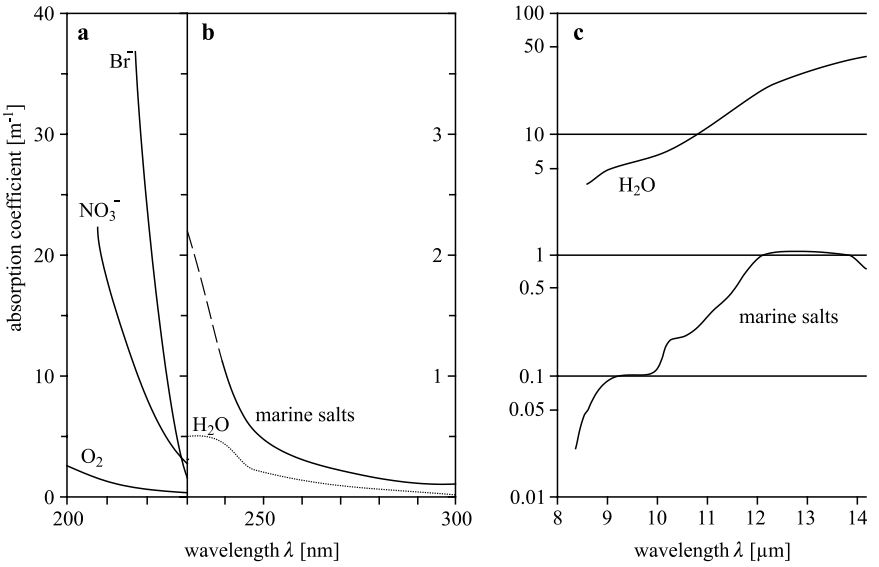

FIGURE 2.16. Comparison of empirical absorption spectra of the principal inorganic absorbers contained in sea water with the absorption spectra of pure water in the UV (a) and (b) and IR regions (c): (a) absorption by aqueous solutions containing: bromide ions Br^- of concentration 65 $mg \cdot dm^{-3}$, nitrate ions NO_3^- of concentration 10 $\mu mol \cdot dm^{-3}$ and dissolved oxygen O_2, of concentration 5 $mg \cdot dm^{-3}$; for the spectral region $\lambda < 230$ nm (after Ivanoff (1978)). (b) Absorption by dissolved salts from the Mediterranean Sea (salinity 37.8 PSU) (after Copin-Montegut et al. (1971)) and absorption by pure water (after Kopelevitch (1983)). Note that empirical data for UV absorption by water are rather inexact (Lenoble and Saint Guily 1955, Morel 1974, Smith and Baker 1981). (c) Absorption of all sea salts in model sea water (salinity 34.8 PSU) and the absorption of pure water. (After empirical data from numerous authors, gathered by Popov et al. (1979).)

estimates of the mass specific coefficients of UV and IR absorption by the major inorganic absorbers in sea water are given in Table 2.16. Any inaccuracies in this context are due to the broad scatter of the empirical data given in the literature, a situation which, in turn, results from the serious technical difficulties involved in the measurement of these coefficients (e.g., the problem of preparing suitably pure samples for spectral analysis, measurements of optical coefficients very low in value, around the detection limit of the spectrometer, etc.).

As can be seen from Table 2.16 and Figure 2.16, two groups of absorbents stand out among the dissolved inorganic substances—dissolved gases and sea salts—which actually or potentially affect the absorption properties of sea water. Moreover, in some cases (strongly mineralized waters), the absorption spectra can also be modified by the absorption of radiation by complexes of transition metal ions. We now discuss in turn the absorption properties of these three groups of absorbers.

2.3.1 Dissolved Gases

During the interaction between the sea and the air, atmospheric gases (oxygen O_2, nitrogen N_2, carbon dioxide CO_2, etc.) and a variety of chemical compounds contained in the aerosol enter the upper layers of the sea, where some of them are dissolved, and the remainder are present in the form of bubbles or suspensions (e.g., Dera (2003)). The small quantities of gases dissolved in sea water are of prime significance for the organisms inhabiting the sea and control of the rates of numerous geophysical processes (Vinogradov 1968, Hansell et al. 2002). But they have little if any effect on the optical properties of ocean waters, unless we take into account the wind-roughened, foam-covered surface of the sea. An exception to this rule is dissolved oxygen O_2: absorption by this is detectable in the UV region below 260 nm (see the O_2 curve in Figure 2.16).

The effect of this band on the overall absorption of radiation by dissolved inorganic substances is usually small; it is apparent mostly in the surface layers of well-aerated waters (Ivanoff 1978, Copin-Montegut et al. 1971).

2.3.2 Salts

In contrast to dissolved gases, it is the soluble salts of certain elements (see Table 2.15) and insoluble H_3BO_3 that make the principal contribution of the inorganic substances dissolved in sea water to the absorption of electromagnetic radiation (Jerlov 1976). The main components of these salts are NaCl, KCl, MgCl, $MgSO_4$, and $CaSO_4$. In open oceanic waters, the concentrations of these compounds (total average concentration = 34.7 $g \cdot dm^{-3}$) and their relative proportions are temporally and spatially extremely stable (Tables 2.17 and 2.18; Dera (2003)).

TABLE 2.16. Spectral mass-specific light absorption coefficients of the major inorganic absorbers in sea water.[a]

A. UV Region

1	Wavelength λ [nm]	200	210	220	230	240	250
-1-	*-2-*	*-3-*	*-4-*	*-5-*	*-6-*	*-7-*	*-8-*
2	Dissolved oxygen O_2 $a^*_{O_2}$ $[m^2g^{-1}]$	0.46	0.18	0.10	0.07	~ 0	—
3	Bromide ions Br^- $a^*_{Br^-}$ $[m^2g^{-1}]$	—	~1.0	0.40	0.014	~ 0	—
4	Nitrates NO^-_3 $a^*_{NO_3}$ $[m^2g^{-1}]$	~40	29,8	13.0	3.2	~ 0	—
5	All salts a^*_S $[m^2g^{-1}]$	1.8×10^{-4}	1.1×10^{-4}	8.0×10^{-5}	5.5×10^{-5}	2.8×10^{-5}	1.2×10^{-5}
6	Percentage[b] [%]		> 80			~ 70	

1	260	270	280	290	300	400
-1-	*-9-*	*-10-*	*-11-*	*-12-*	*-13-*	*-14-*
5	8.1×10^{-6}	5.7×10^{-6}	4.0×10^{-6}	2.9×10^{-6}	2.6×10^{-6}	$< 1\times10^{-7}$
6			~ 70			< 10

B. IR Region

1	Wavelength λ [μm]	1.5–9.0	9.0	9.4	9.8	10.2	10.6	11.0
-1-	*-2-*	*-3-*	*-4-*	*-5-*	*-6-*	*-7-*	*-8-*	*-9-*
2	All salts a^*_S $[m^2g^{-1}]$	~ 0	2.9×10^{-6}	2.9×10^{-6}	2.9×10^{-6}	5.7×10^{-6}	5.7×10^{-6}	8.6×10^{-6}
3	Percentage[b] [%]	~ 0	2	1.9	1.7	2.9	2.4	2.8

1	11.8	12.3	12.6	13.0	13.4	13.8	14.2	14.6	15.5
-1-	*-10-*	*-11-*	*-12-*	*-13-*	*-14-*	*-15-*	*-16-*	*-17-*	*-18-*
2	1.1×10^{-5}	2.0×10^{-5}	2.9×10^{-5}	2.9×10^{-5}	2.9×10^{-5}	2.6×10^{-5}	2.4×10^{-5}	2.0×10^{-5}	1.7×10^{-5}
3	2.8	3.8	4.3	3.1	2.8	2.4	2.0	1.7	1.4

[a] Estimated on the basis of empirical data obtained from the following papers: Popov et al. (1979), Ivanoff (1978), Copin-Montegut et al. (1971), Armstrong and Boalch (1961), Kopelevich and Shifrin (1981), and Kopelevitch (1983).

[b] In Tables A (line 6) and B (line 3) we give the approximate percentage of absorption by the salt in the total absorption of light by model artificial sea water (an aqueous solution of all the main sea-salt components) with a salinity of c. 35 PSU, that is, typical of open ocean water.

At the same time, the salts listed in Table 2.18 are by weight the second largest group of sea water components after the water itself. In addition, nutrient salts, nitrates in particular (also listed in Table 2.18), although present in lower concentrations than the salts mentioned earlier, are also to some extent optically significant. Their concentrations fluctuate considerably in time, however, and are spatially extremely variable (e.g., Popov et al. (1979)).

When interacting with the strongly polar molecules of water, these dissolved mineral salts dissociate into positive metal ions and negative acid residues. The nondissociating H_3BO_3 is exceptional in this respect. As a result

TABLE 2.17. Occurrence and functions of the principal constituents of sea water in the World Ocean.

Constituent	Source literature	Total content in the world ocean (tons)	% of Total mass	Mean concentration [$\mu g \cdot dm^{-3}$]	Principal biological and optical functions
-1-	*-2-*	*-3-*	*-4-*	*-5-*	*-6-*
Water	Ivanenkov 1979a	1.36×10^{18}	96.6	9.92×10^{5}	The environment of life; sources of tissue fluids, Hydrogen and Oxygen; light absorption and scattering.
Total admixtures	Ivanenkov 1979a	4.78×10^{16}	3.40	3.49×10^{4}	
Ions of the principal salts					
Cl^-, Na^+, Mg^{2+}, SO_4^{2-}, Ca^{2+}, K^+, Br^-, HCO_3^-, Sr^{2+}, F^{2-}, H_3BO_3	Ivanenkov 1979a	4.78×10^{16}	3.40	3.49×10^{4}	Source of catalytic and some structural nutrients (low biological activity); optically practically inactive.
Trace elements					
Li, Rb, P, I, Ba, Mo, Fe, Zn, As, V, Cu, Al, Ti	Ivanenkov 1979a	3.00×10^{11}	2.13×10^{-5}	2.19×10^{-1}	
Other trace elements					
(c. 50 elements)	Ivanenkov 1979a	3.00×10^{10}	2.13×10^{-6}	2.308×10^{-2}	
Biologically active					
Dissolved gases					
N_2, O_2, CO_2, Ar	Ivanenkov 1979a	3.24×10^{13}	2.30×10^{-3}	2.36×10^{1}	O_2, CO_2: sources of oxygen and carbon; optically inactive.
Inorganic nutrients					
C	Alekin 1966	1.15×10^{14}	8.17×10^{-3}	8.27×10^{1}	Active sources of nutrients; optically inactive.
Si	Vinogradov 1967	3.60×10^{13}	2.55×10^{-3}	2.59×10^{1}	
N	Ivanenkov 1979b	2.90×10^{12}	2.06×10^{-4}	2.08	
P	Vaccaro 1965	5.80×10^{11}	4.12×10^{-5}	4.17×10^{-1}	
	Ivanenkov 1979b	9.90×10^{10}	7.04×10^{-6}	7.12×10^{-2}	

(*Continued*)

TABLE 2.17. Occurrence and functions of the principal constituents of sea water in the World Ocean.— Cont'd.

Constituent	Source literature	Total content in the world ocean (tons)	% of Total mass	Mean concentration [$\mu g \cdot dm^{-3}$]	Principal biological and optical functions
-1-	*-2-*	*-3-*	*-4-*	*-5-*	*-6-*
Optically active					
Organic substances in organisms					
Total[a]	Alekin 1966	6.00×10^{10}	4.26×10^{-6}	4.32×10^{-2}	Fountain of life; potential sources of nutrients; absorption and scattering.
	Bogorov 1968	3.30×10^{9}	2.36×10^{-7}	2.37×10^{-3}	
Chlorophyll	Whittaker & Likens 1975	1.8×10^{7}	1.28×10^{-9}	1.29×10^{-5}	
Organic substances in the environment					Potential or active sources of nutrients; light absorption and scattering.
(dissolved + suspended)[a]	Alekin 1966	2.00×10^{13}	1.42×10^{-3}	1.43×10^{1}	
	Skopintsev 1971	4.00×10^{12}	2.84×10^{-4}	2.88	

[a] The resources of inorganic carbon and the diverse forms of organic matter have been variously assessed by different authors. The relevant extreme values are given in the tables.

Table 2.18. Approximate average concentrations in ocean water of the principal salt anions and cations, and also nitrates.

Ion or Molecule	Average Concentration in ‰ by Weight[a]
Principal Salts	
Cl^-	18.98
SO_4^{2-}	2.65
HCO_3^-	0.139
Br^-	0.065
F^-	0.001
Na^+	10.56
Mg^{2+}	1.27
Ca^{2+}	0.40
K^+	0.38
Sr^{2+}	0.013
H_3BO_3	0.005
Nitrates	
NO_3^-	0.0015

[a] Based on data given by Popov et al. (1979), Vaccaro (1965), Ivanov (1975), and Brown et al. (1989).

of the change in their electronic, oscillational, and rotational states, neutral molecules and inorganic ions absorb radiation in various regions of the electromagnetic spectrum. Lenoble (1956) and Copin-Montegut et al. (1971) demonstrated empirically that the absorption of radiation by aqueous solutions of most of these fundamental mineral components of sea water takes place mainly in the ultraviolet region of the spectrum (230–300 nm; see Figure 2.16). The absorbed quanta of radiation induce a change in the electronic oscillational-rotational state of the ion or molecule, and in doing so, give rise to an absorption band of varying breadth and intensity. The intensity of these absorption bands in the UV region rises monotonically with the increase in the energy of the interacting quanta, that is, with a fall in wavelength (Armstrong and Boalch 1961). The further rise in the absorption coefficients in the $\lambda \in$ 230–300 nm region is due largely to the bromide ion Br^- (Ogura and Hanya 1967) (the Br^- curve in Figure 2.16). Nitrate ions NO_3^- can also absorb strongly in this region (the NO_3^- curve in Figure 2.16). Below 200 nm, the empirical spectra of radiation absorption by sea water components have not been subjected to detailed scrutiny. It should be noted further that the coefficients of UV light absorption by sea salts are larger in value than the corresponding coefficients for water molecules. (Figure 2.16b). So in this region, the percentage share of salts in the total absorption of radiation in model (artificial) sea water of salinity 35 PSU is from 70 to >80% (see line 6 in Table 2.16). In less saline waters this value will, of course, be proportionally less.

The IR absorption properties of sea salts have been characterized by Friedman (1969), Pinkley and Williams (1976), and Pinkley et al. (1977), among others. These authors have shown that mineral salts and their ions absorb IR radiation mainly in the wavelength interval $9 < \lambda < 15$ μm (Figure 2.16c), forming oscillational-rotational absorption bands consisting of numerous overlapping spectral lines. The intensity of these bands, however, is weak, far more so than that of the corresponding bands for the water itself. As we can see from line 3 in Table 2.16B, the contribution of salts to the total absorption of IR radiation in sea water of salinity 35 PSU is no more than a few percent. As a result, these bands are practically invisible against the background of the IR absorption band of water. That is why the empirical spectrum of IR absorption by sea water is practically identical in all seas, that is, is independent of salinity.

As far as visible radiation is concerned, solutions of mineral salts behave as if they were optically transparent; that is, they transmit the entire range of the VIS spectrum, with hardly any being lost through absorption. For one thing, this is because none of the metals in the principal components of sea salt are spectrally active, either in the visible or in the near ultraviolet (see Table 2.15). What is significant, however, is that salts exert an important influence on the molecular scattering of light in sea water: in oceanic waters the components of sea salt are responsible for c. 30% of the scattering due to all the molecules present in sea water (Morel 1974, Kopelevitch 1983).

2.3.3 Inorganic Complex Ions

Mineral salts and dissolved gases have practically no effect on the absorption properties of sea water with respect to visible radiation: this is a characteristic feature of the vast majority of sea and oceanic waters. Nevertheless, Kondratev and Pozdniakov (1988) have shown that such an effect can be detected in highly mineralized waters, such as saline lakes with high concentrations of transition metals,[21] mostly manganese and iron (Alekin 1970, Kondratev et al. 1990). Ions of these metals absorb visible light (Table 2.15). Moreover, under appropriate environmental conditions (suitable pH and temperature), these ions can form complexes with water molecules and other inorganic compounds that function as ligands. Complex formation between metals and ligands can potentiate absorption capabilities of the former. The basic theory of the absorption spectra of such complexes can be found, for example, in Gołębiewski (1982), Babko and Pilipienko (1972), and Barrow (1969). Figure 2.17 illustrates visible extinction spectra $\varepsilon(\lambda)$[22] of aqua-complexes of manganese and nickel.

---

[21] For example, the average mineralization of Lake Ladoga is 56 $mg \cdot dm^{-3}$ (after Raspletina et al. (1967)), whereas the metal content in Lake Balkhash near the mouth of the river Ili may be several times greater (Alekin 1970).

[22] See the definition of ε in the footnote 2 to Chapter 3.

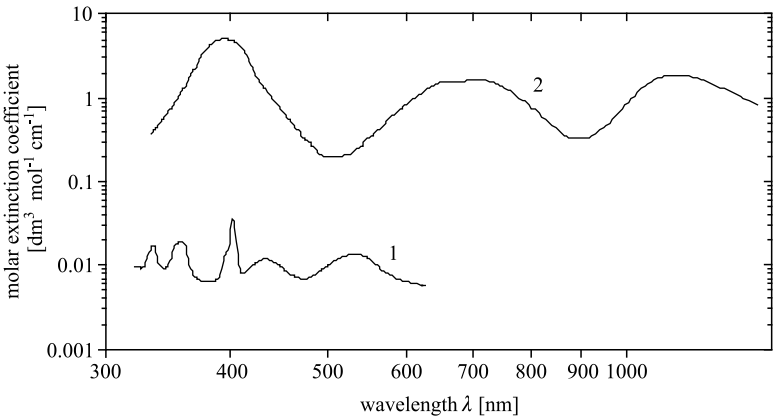

FIGURE 2.17. Spectra of molar extinction coefficients ε for aqua-complexes of manganese ($[Mn(H_2O)_6]^{2+}$) (1) and nickel ($[Ni(H_2O)_6]^{2+}$) (2). (Data from Barrow (1969).)

TABLE 2.19. Absorption band peaks (λ_{max}) and colors of selected complex ions.[a]

Complex	λ_{max} [mn]	Color
-1-	*-2-*	*-4-*
$[Co(CN)_6]^{3-}$	300	Colorless
$[Co(NH_3)_6]^{3+}$	330, 470	Yellow red
$[Cr(H_2O)_6]^{3+}$	405, 580	Purple
$[Ti(H_2O)_6]^{3+}$	545	Purple red
$[Co(H_2O)_6]^{2+}$	500, 900	Pink
$[CoCl_4]^{2-}$	665	Blue
$[Cu(NH_3)_4]^{2+}$	640	Blue
$[Cu(H_2O)_6]^{2+}$	790	Pale blue
$[Ni(H_2O)_6]^{2+}$	500, 705, 880	Green
$[Mn(H_2O)_6]^{2+}$	305, 350, 400, 465, 555	Very pale pink

[a] Data taken from Phillips and Williams (1966); see also Campbell and Dwek (1984).

Table 2.19 gives the rough positions of absorption band peaks and the colors of selected complexes of transition metals with inorganic ligands. This absorption can cause a change in the color of natural waters, especially of inland waters, whose optical properties are far more complicated and much less well understood that those of sea waters. Nonetheless, the effects just described may well occur in certain regions of the sea, although on a smaller scale. Unfortunately, however, we are not aware of any papers that can provide confirmation of this.